

## Mineralogical and Geochemical Evidence for Granite Metasomatism in Dikes in the North of the Berezovskoe Ore Field (Middle Urals)

S.Yu. Stepanov<sup>a,✉</sup>, E.S. Shagalov<sup>a</sup>, R.S. Palamarchuk<sup>b</sup>, A.V. Kuttyrev<sup>c</sup>,  
L.N. Sharpenok<sup>d</sup>, F.M. Nabiullin<sup>e</sup>, A.N. Troshkina<sup>e</sup>

<sup>a</sup> Zavaritsky Institute of Geology and Geochemistry, Ural Branch of the Russian Academy of Sciences,  
ul. Akademika Vonsovskogo 14, Yekaterinburg, 620016, Russia

<sup>b</sup> South Urals Federal Research Center of Mineralogy and Geoecology, Ural Branch of the Russian Academy of Sciences,  
territory of the Ilmeny State Reserve, Miass, Chelyabinsk Region, 456317, Russia

<sup>c</sup> Institute of Volcanology and Seismology, Far Eastern Branch of the Russian Academy of Sciences,  
bul'v. Piipa 9, Petropavlovsk-Kamchatsky, 683006, Russia

<sup>d</sup> A.P. Karpinsky Russian Geological Research Institute, Srednii prosp. 74, St. Petersburg, 199106, Russia

<sup>e</sup> OOO Berezovskii Rudnik, ul. Berezovskii trakt 1, Berezovskii, Sverdlovsk Region, 623703, Russia

Received 4 December 2018; received in revised form 15 October 2019; accepted 27 November 2019

**Abstract**—We present results of petrographic, geochemical, and mineralogical studies of apogranite metasomatites associated with sulfide–quartz gold ore veins. The studies show a predominance of muscovite and quartz–muscovite metasomatites. Formation of muscovite metasomatites was accompanied by the accumulation of W, Sc, Zr, Hf, Ga, REE, U, Th, Ta, and Nb and the genesis of new accessory minerals: monazite-(Ce), apatite, zircon, scheelite, W-containing rutile, uraninite, thorianite, cassiterite, etc. Compared with the primary granites, quartz–muscovite metasomatites are richer in Pb, Bi, As, Sb, Co, Ni, Ba, In, Cd, Mo, Te, Ag, and Au (elements of the gold ore assemblage). The high contents of these trace elements are due to abundant galena, fahlores, chalcopyrite, and pyrite among the accessory minerals. Metasomatism of granites was followed by the removal of SiO<sub>2</sub>, which was then spent for the formation of quartz veins. We have revealed that the distribution of metasomatites of different types within a dike body affects directly the distribution of sulfide–quartz veins and thus determines the ore content of the dike body fragments.

**Keywords:** gold deposits, geochemical gold mineral assemblage, REE, apogranite metasomatites, Middle Urals, Berezovskoe ore field

### INTRODUCTION

The Berezovskoe gold deposit is one of the oldest primary gold deposits in Russia but is still exploited. Until the 1970s, the main mining work at the deposit was performed at depths of up to 200 m. In the second half of the 20th century, during the prospecting work of the Uralzoloto Trust supervised by V.F. Kazemirskii, gold reserves in the lower horizons of the Berezovskoe ore field in metasomatized granite dikes were evaluated. These dikes are penetrated by sulfide–quartz veins forming systems of ladder veins. At present, it is dikes with numerous sulfide–quartz veins that are of the main commercial interest.

At the early stages of development of the Berezovskoe deposit, its minerals, rocks, and ores were studied by Rose (1842), Karpinskii (1887), and Obruchev (unpublished

data). Detailed research was performed at the mine in the 1960–1970s (Bellavin et al., 1970; Popov, 1970, 1971; Samartsev et al., 1973; Chesnokov et al., 1976; Kurulenko, 1977). The use of modern high-precision (including isotope) investigation methods made it possible to study the ores of the Berezovskoe deposit in detail (Sazonov, 1984; Bortnikov et al., 1998; Baksheev et al., 2001; Pribavkin, 2002; Sazonov et al., 2006, 2009; Baksheev and Belyatskii, 2011; Spiridonov et al., 2013; Vikent'eva et al., 2017; Pribavkin et al., 2018). Most of the researchers focused on different types of ore-bearing quartz veins and studied primarily gold ore parageneses. There were also investigations concerned with the input and removal of major rock components (Borodaevskaya, 1944; Borodaevskii and Borodaevskaya, 1947; Grabezhev, 1970; Popov, 1971) and trace elements (Sazonov et al., 2006, 2009) during the metasomatic transformation of granitoids and the host rocks. The research was aimed mainly at the comprehensive description of mineral assemblages in the already explored parts of the ore field. The influence of metasomatites on the input and removal of elements and

✉ Corresponding author.

E-mail address: Stepanov-1@yandex.ru (S.Yu. Stepanov)

the relationship of their different types with ore formation were not examined for the ore blocks with a rather even distribution of sulfide–quartz veins and gold. However, the progressive exploitation of the deposit to depth, especially in the northern part of the Berezovskoe ore field, reveals an increasingly uneven distribution of gold in blocks and a more contrasting manifestation of apogranite metasomatites, which differ significantly from other metasomatic rocks in mineral composition and spatial relationship with sulfide–quartz veins. The combination of these facts calls for a new research into apogranite metasomatites and elucidation of the spatial and genetic relationship of their mineral assemblages with gold mineralization.

In this work we performed the first geochemical studies of the trace-element composition of all major varieties of apogranite metasomatites from the northern part of the Berezovskoe ore field and confirmed the results by a detailed analysis of the hosted minerals.

The goal of the research was to elucidate the relationship between apogranite metasomatites of different types and gold mineralization, based on the established regularities of changes in mineral composition and migration of rock-forming and trace elements during the metasomatic process. The research included solution of the following problems: elucidation of the spatial and temporal regularities of localization of apogranite metasomatites and sulfide–quartz veins, based on the results of a study of mine workings in the ore field; comprehensive petrographic and geochemical study of metasomatites and granites; and identification of minerals concentrating trace elements in granites and metasomatites.

## SAMPLES AND METHODS

Studies were carried out for rocks from the Il'inskaya, Andreevskaya, and Vtoropavlovskaya dikes (granite-porphry) and from the Sevast'yanovskaya, Pervopavlovskaya, and Elizavetinskaya dikes (plagiogranite-porphry) penetrated by prospecting drifts, in some of which fragments accessible for geological observations reached 1400 m in length (Andreevskaya dike, horizon –412 m). A preliminary study of metasomatites and sulfide–quartz veins occurring at different depths and at different distances from an intrusive body (Shartash massif) did not reveal a metasomatic zoning or a systematic change in metasomatic and ore mineral assemblages. Based on the results of numerous geological observations in the workings of the Northern and Central mines, we selected and documented fragments of dike bodies with metasomatites of different types and quartz veins. Samples for petrographic studies and chemical analyses were taken both from unaltered granites and from apogranite metasomatites of all types found on the walls of mine workings in horizons from –512 to –162 m, with a total of 134 lump samples. The samples were used to prepare standard petrographic thin sections (185), transparent polished thin sections (123), and polished sections (89).

Impurity-concentrating accessory minerals from granites and metasomatites were identified and examined by scanning electron microscopy and X-ray probe microanalysis. The polished samples were studied with CamScan MX2500 (Russian Geological Research Institute, St. Petersburg, analyst A.V. Antonov) and JEOL-JSM6390LV (Institute of Geology and Geochemistry, Yekaterinburg, analyst E.S. Shagalov) scanning electron microscopes. The composition of minerals was determined on a Link Pentafet (Oxford Instruments) EMF spectrometer with a Si(Li) detector with an area of 10 mm<sup>2</sup> and a resolution of 138 eV (MnK<sub>α</sub> radiation). Before the study, the surface of polished samples was sprayed with carbon. Probe microanalysis conditions: accelerating voltage of 20 kV, working distance of 35 mm, probe current (on the Faraday cup) of 0.5 nA, XPP correction of matrix effects (INCA Energy software), and integration time of 70 s (ignoring the dead time equal to 25–40% of the total analysis time). Control of measurements was made by analysis of chemically pure cobalt every 2 h. The electron beam (on the Faraday cup) drifted within 3–5% of the initial value for this time. The following certified natural and synthetic materials were used as standards: Cu – Cu<sub>met</sub>; Fe – Fe<sub>met</sub>; Ni – Ni<sub>met</sub>; Co – CoAsS; S – FeS<sub>2synth</sub>; As – InAs; Sb – CuSbS<sub>2</sub>; Te, Pb – PbTe; and Bi – Bi<sub>met</sub>. The detection limits for elements were as follows (wt.%): Fe – 0.03, Ni – 0.03, Cu – 0.03, S – 0.05, As – 0.05, Co – 0.03, Pb – 0.08, and Bi – 0.10.

The contents of microimpurities in the primary granites and metasomatites were determined on an ELAN-DRC-6100 quadrupole mass spectrometer with inductively coupled plasma (Russian Geological Research Institute, St. Petersburg, analysts V.A. Shishlov and V.L. Kudryashov). The content of As in the samples was determined after their digestion in aqua regia, and the contents of Se, Te, Ge, Cd, Ag, Sc, Tl, Bi, Ni, Co, Cu, Zn, Pb, and In, after their complete acid decomposition. Analysis for REE, Cr, V, Ti, Rb, Sr, Y, Zr, Ba, W, Sn, and Mo was carried out after the fusion of the samples. The detection limits for the elements were as follows (ppm): Ba – 3, V – 2.5, Rb – 2, Cr, Ni, Cu, Zn, Pb, Li, Be, and Sr – 1, Mo – 0.6, Co, Zr, Nb, Te, W – 0.5, Se – 0.3, Sn – 0.2, Ga, Ge, Y, Cd, Sb, Cs, Ta, Tl, Bi, Th, U, As – 0.1, and REE, Hf, Ag – 0.01. The content of Hg in the rocks was determined by the cold-steam method on a Perkin Elmer AAnalyst 800 atomic-absorption spectrometer; the detection limit for Hg was 0.01 ppm. The content of Au was determined on a Perkin Elmer AAnalyst 600 atomic-absorption spectrometer; the detection limit for Au was 0.002 ppm. The content of S was measured with an AC-7932 analyzer; the detection limit for S was 0.01%. The contents of rock-forming components were determined by approximate quantitative atomic-emission spectral analysis; the detection limits were 0.01% for most of the components, 0.001% for TiO<sub>2</sub>, and 0.0002% for MnO. The determined contents of trace elements in granites and metasomatites were grouped based on the nomenclature proposed by Sklyarov et al. (2001).

## THE STRUCTURE OF THE BEREZOVSKOE ORE FIELD

The Berezovskoe ore field is located northeast of the Shartash granite massif (Fig. 1) of the Carboniferous Verkhnyaya (Upper) Iset' complex (Pribavkin et al., 2013). Within

the ore field, the roof of the intrusion gradually dips to the northeast (Bellavin et al., 1970), toward the area of volcanics and volcanosedimentary rocks of the Ordovician Novaya Berezovka Formation with thrust sheets of Ordovician ultramafic rocks of the Pervomaiskii complex. The rocks of the Novaya Berezovka Formation and the Pervomaiskii

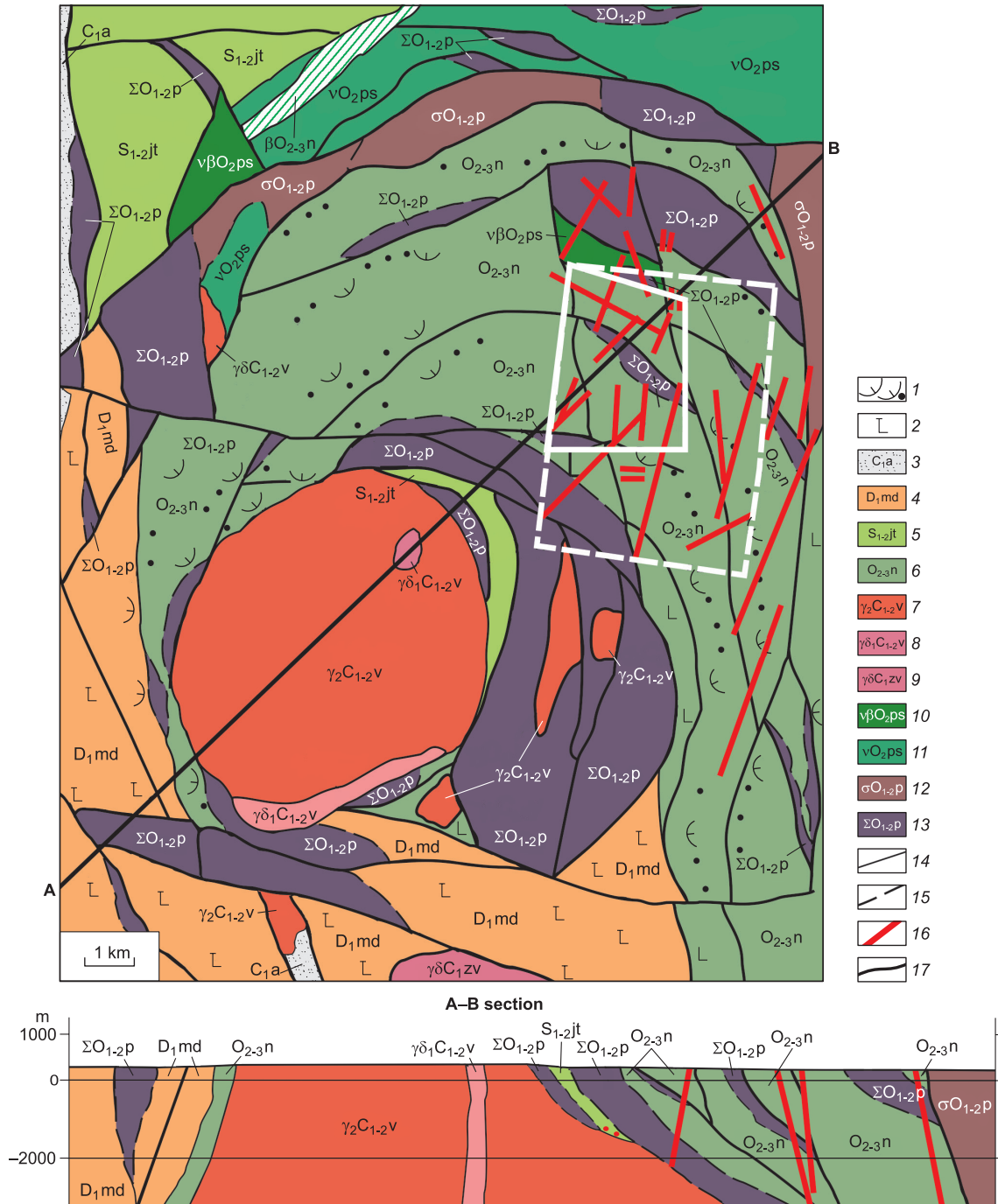


**Fig. 1.** Geologic structure of the Berezovskoe ore field, after Bellavin et al. (1970) and Kalugin et al. (2017). Volcanosedimentary rocks (1, tuffs and tuffstones, 2, basalts); 3, sandstones of the Aramil' Formation; 4, basalts and tuffs of the Medvedevka Formation; 5, rocks of siliceous-terrigenous strata; 6, basalts, tuffs, and tuffites of the Novaya Berezovka Formation; intrusive rocks: Verkhnyaya Iset' complex (7, granites; 8, granodiorites), Western Verkhnyaya Iset' complex (9, granodiorites), Pyshma complex (10, gabbro-dolerites; 11, gabbro), Pervomaiskii complex (12, peridotites; 13, ultramafites); contacts: 14, conformable or intrusive; 15, tectonic; 16, granite dikes; 17, large faults.

complex are cut by granite dikes of the third intrusion phase of the Shartash massif (Kurulenko, 1977).

Based on the geologic structure of the Berezovskoe ore field, the specific composition of its ore and vein minerals, and the results of isotope research and study of gas–liquid inclusions, most researchers classify the Berezovskoe gold deposit with diverse types of ores (including scheelite mineralization (Kurulenko et al., 1984)) as a typical plutonic–hydrothermal object with a magmatogene fluid playing the leading role in the ore formation (Bortnikov et al., 1998; Baksheev et al., 2001; Baksheev and Belyatskii, 2011; Vikent’eva et al., 2017). The relationship among metasomatic processes, ore formation, and the intrusion of the Shartash massif granitoids is confirmed by the endogenous zoning of the ore field, expressed as a change in mineral assemblages (Chesnokov, 1973; Chesnokov et al., 1976), dominating types of metasomatites (Borodaevskii and Borodaevskaya, 1947; Popov, 1970), and ore mineral assemblages (Samartsev et al., 1973) with distance from the intrusive body.

According to the international classification, the Berezovskoe deposit can be referred to as an intrusion-related gold deposit. It is similar to the Palpa-Ocoña Au–As–Pb–Zn–Cu–Ag deposit with numerous sulfide–quartz veins in Peru (Schreiber et al., 1990; Sillitoe and Thompson, 1998), the Vasil’kovskoe deposit in Kazakhstan (Thompson et al., 1999), and gold deposits in the Tintina Gold Province in the North American Cordillera (Hart and Goldfarb, 2005).

The geologic structure of the Berezovskoe ore field is described in detail elsewhere (Borodaevskii and Borodaevs-

kaya, 1947; Polenov et al., 2013; Pribavkin et al., 2013; Vikent’eva et al., 2017). A specific feature of the field is the occurrence of granite dikes as two linearly stretching zones in volcanosedimentary rocks of the Novaya Berezovka Formation and in serpentinites of the Pervomaiskii complex, which merge along the dip. Both the granite dikes and the host rocks underwent significant metasomatic transformations to form “ladder” (in granite dikes) and “krassyyk” (in the host rocks) quartz veins.

The unaltered granite-porphyry and plagiogranite-porphyry of dikes are rocks with an equigranular texture composed of plagioclase (oligoclase Nos. 25–30), alkali feldspar, quartz, and rare biotite phenocrysts, amounting to 50 vol.%. The rock groundmass is a fine- to thin-grained aggregate of plagioclase, alkali feldspar, and quartz. However, plagiogranite-porphyry contains much less quartz and alkali feldspar, up to the absence of the latter. Phenocrysts in it amount, on average, to  $\leq 40$ –45%. The groundmass of plagiogranite-porphyry is similar to that of granite-porphyry but shows a clear predominance of plagioclase.

## RESULTS

**Petrographic and petrochemical evidence for granite alterations during metasomatic processes.** The petrographic study of thin sections of unaltered and metasomatized granites has shown that biotite was among the first to be replaced by a muscovite aggregate (Fig. 2). Then, plagi-

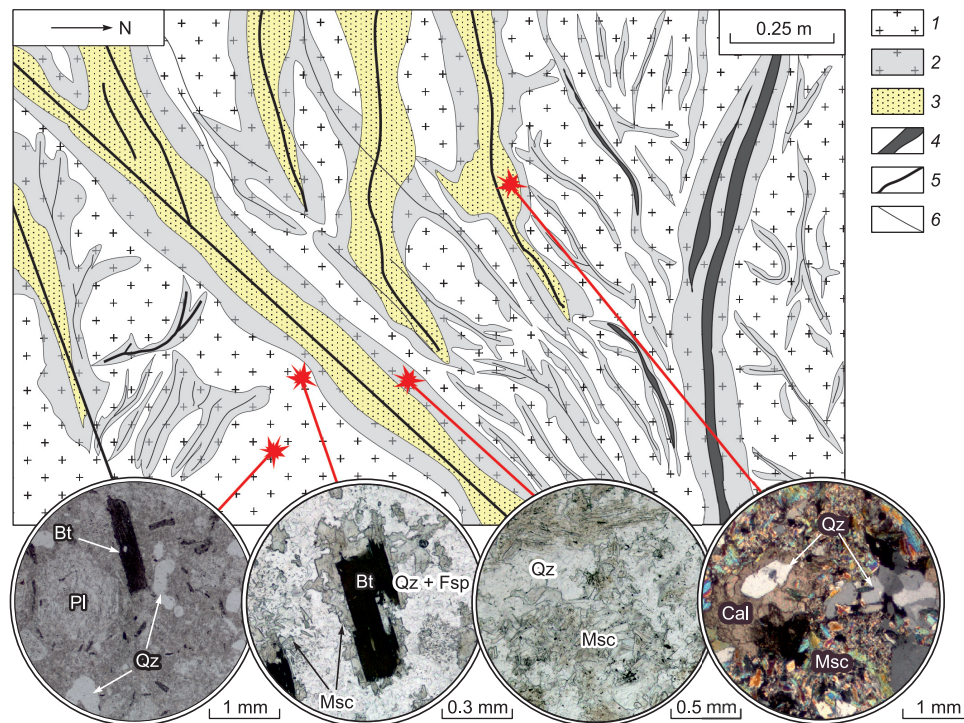


**Fig. 2.** Scheme of the wall of a drift along the Andreevskaya dike, with photomicrographs of the thin sections of granites and metasomatites. 1, weakly altered granite-porphyry; 2, granite-porphyry replaced by quartz–muscovite aggregate; 3, muscovite metasomatites; 4, quartz veins; 5, large faults; 6, small fractures. Bt, biotite, Pl, plagioclase, Qz, quartz, Msc, muscovite, Fsp, K–Na-feldspar, Cal, carbonate.

clase and K–Na-feldspars were replaced by quartz–muscovite aggregate. Quartz phenocrysts were the last to undergo metasomatic replacement. Fine- to medium-grained quartz–muscovite aggregate or muscovite metasomatites were the final products of granite alteration. The aggregate contains numerous pyrite metacrysts and subordinate carbonates. Such metasomatites occur mostly near the contacts of ladder quartz veins, as, for example, in the Andreevskaya and Vtoropavlovskaya dikes.

Medium- to coarse-grained muscovite pegmatites are also widespread. They are localized mostly along fractures filled with calcite, sulfide aggregate, or, very seldom, quartz–carbonate veins. In the Il'inskaya and Vtoropavlovskaya dikes, muscovite metasomatites were observed along quartz and quartz–carbonate veins containing scheelite crystals and aggregates. A specific feature of these metasomatites is high porosity and high content of carbonates (Fe-dolomite and ankerite). Petrographic examination of thin sections showed a maximum porosity of 12.5 vol.%. The pore walls are often composed of a later formed microdruses of calcite (and, seldom, Fe-dolomite). In places, quartz–muscovite aggregate is not localized in large fractures and quartz veins but completely replaces granites (Fig. 3), e.g., at the horizon –342 m of the Il'inskaya dike and at the horizon –362 m of the Sevast'yanovskaya dikes in the northern part of the Berezovskoe ore field.

Thus, the metasomatites developed after dike granites in the northern part of the Berezovskoe ore field can be subdivided

into quartz–muscovite and muscovite ones according to the results of petrographic examinations and geological studies.

The geological observations do not reveal any regularities of the distribution of various metasomatites within granite dikes. The results of petrographic examinations show no significant spatial variations in the mineral composition of apogranite metasomatites, which indicates no metasomatic zoning within the studied site (2.4 km in length and on average 400 m in depth) of the Berezovskoe ore field. The areas of localization of quartz–muscovite and muscovite metasomatites coincide (Fig. 4b, c). We have found zones with widespread muscovite metasomatites within the Andreevskaya and Vtoropavlovskaya dikes (Fig. 4d).

A similar pattern of metasomatic transformation of granites is observed in all studied sections. For this reason, it is necessary to study the distribution of rock-forming and trace elements in granites and metasomatites at local near-vein or near-fracture sites of the sections of metasomatically transformed dikes.

The results of petrochemical studies of the granites show that their metasomatic transformation leads to a significant loss of SiO<sub>2</sub> and Na<sub>2</sub>O (Table 1). The contents of other rock-forming elements are given in supplementary materials ([http://sibran.ru/journals/Stepanov\\_et\\_al\\_Supplementary.docx](http://sibran.ru/journals/Stepanov_et_al_Supplementary.docx)). The average contents of SiO<sub>2</sub> and Na<sub>2</sub>O are, respectively, 72–73 wt.% and 4 wt.% in granites, 65–67 wt.% and 0.15 wt.% in quartz–muscovite metasomatites, and 50–

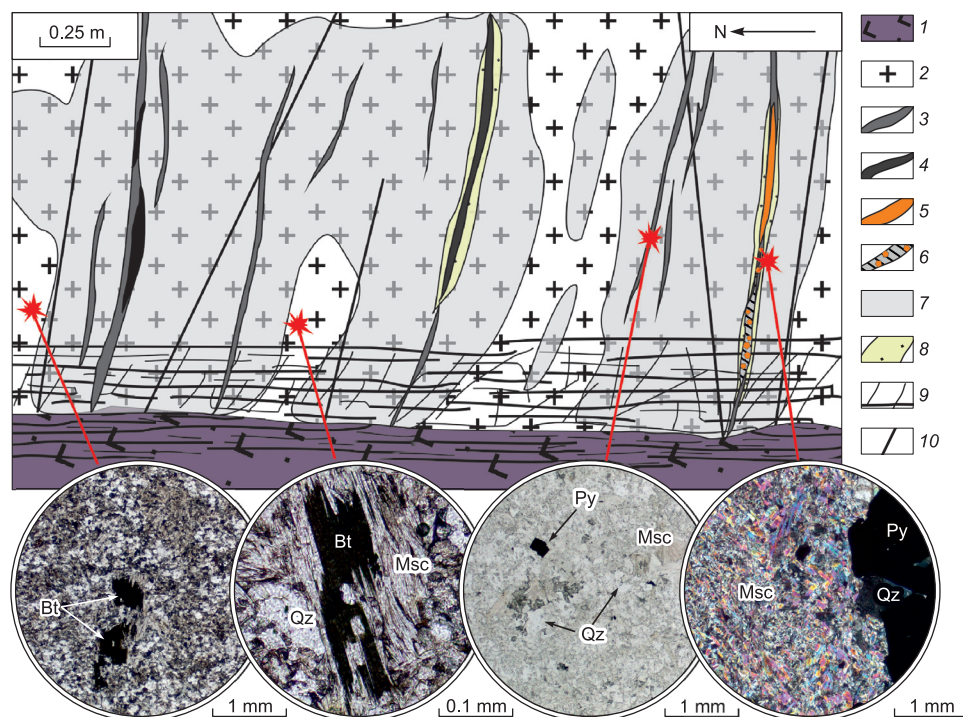


**Fig. 3.** Scheme of the wall of a drift along the Il'inskaya dike, with photomicrographs of the thin sections of granites and metasomatites.

1, listwanitized mafic tuffs and tuffites; 2, granite-porphphy with quartz–muscovite aggregates; 3, quartz veins; 4, prevalent sulfide veins; 5, sites of quartz veins with scheelite aggregates; 6, quartz veins with occasional scheelite crystals; 7, quartz–muscovite metasomatites; 8, muscovite metasomatites; 9, small fractures; 10, large faults. Py, pyrite, other designations follow Fig. 2.

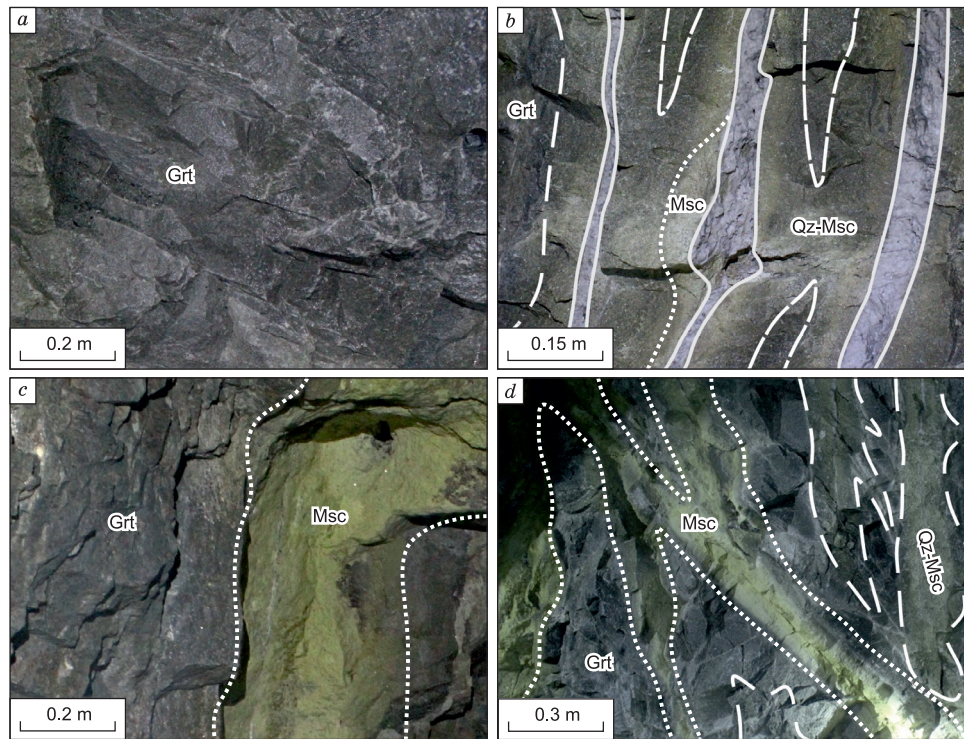


**Fig. 4.** Rocks of the Vtoropavlovskaya dike (*a–c*): *a*, weakly altered granites (Grt); *b*, near-vein quartz–muscovite (Qz–Msc) metasomatites; *c*, near-fracture muscovite (Msc) metasomatites; *d*, arrangement of different metasomatites in the wall of a drift along the Andreevskaya dike. Solid lines are the borders of quartz veins, dashed lines are the borders of zones of quartz–muscovite metasomatites, and dotted lines are the borders of zones of muscovite metasomatites.

54 wt.% and 0.12 wt.% in muscovite metasomatites. The content of  $\text{Na}_2\text{O}$  in the rocks significantly decreases even during weak metasomatic processes, reaching a minimum in both quartz–muscovite and muscovite metasomatites. Changes in the chemical composition of rocks during metasomatism are clearly seen from the calculated change in the amount of the substance of granite-porphphyry from the Vtoropavlovskaya dike during its replacement by quartz–muscovite and muscovite rocks (Table 1). Calculation by Rudnik’s (1962) technique taking into account not only the change in the contents of components but also the change in the volume mass, density, and porosity of rocks yields the total loss of the substance of 3.25 wt.% for quartz–muscovite metasomatites and 10.9 wt.% for muscovite metasomatites, which is correlated with the increase in the rock porosity.

The contents of  $\text{K}_2\text{O}$  and  $\text{Al}_2\text{O}_3$  in both types of metasomatites are significantly higher compared with the unaltered granites (Table 1). In addition, muscovite metasomatites have much higher CaO contents. The input of major rock-forming components changes the mineral composition of the rocks and is accompanied by the formation of muscovite and carbonates (Fe-dolomite and calcite) in metasomatites of both types.

**Indicators of geochemical processes during granite metasomatism.** The REE patterns of granites and metasomatites (Fig. 5) have much in common. Granites from different dikes show similar negatively sloped REE patterns with

no Eu anomaly (Fig. 5*a*). The REE contents are given in supplementary materials ([http://sibran.ru/journals/Stepanov\\_et\\_al\\_Supplementary.docx](http://sibran.ru/journals/Stepanov_et_al_Supplementary.docx)). Both quartz–muscovite (Fig. 5*b*) and muscovite (Fig. 5*c*) metasomatites have higher contents of LREE as compared with unaltered granites but similar HREE contents. Comparison of the REE patterns of rocks from the Andreevskaya and Vtoropavlovskaya dikes (Fig. 5*d, e*) shows a regular increase in the REE contents of metasomatites relative to those of unaltered granites. Moreover, muscovite metasomatites from the Andreevskaya dike are richer in HREE as compared with quartz–muscovite metasomatites. Rocks from the Vtoropavlovskaya dike show opposite REE patterns. All studied metasomatic rocks tend to accumulate REE (Fig. 5*f*): Muscovite metasomatites are enriched in LREE, and quartz–muscovite ones, in HREE.

The HFSE contents (Fig. 6) in granites and metasomatites are nearly the same, but the granites are slightly enriched in Th, U, Ta, and Nb. The HFSE patterns of quartz–muscovite metasomatites (Fig. 6*b*) are identical to those of unaltered granites. Muscovite metasomatites are enriched in Th, U, Y, Zr, Hf, Nb, and Ta relative to granites and quartz–muscovite metasomatites. We did not reveal a relationship between the HFSE contents in granites and metasomatites and the localization of these rocks within the ore field. The HFSE contents are given in supplementary materials ([http://sibran.ru/journals/Stepanov\\_et\\_al\\_Supplementary.docx](http://sibran.ru/journals/Stepanov_et_al_Supplementary.docx)).

**Table 1.** Changes in the amount of the substance of plagiogranite-porphry from the Vtoropavlovskaya dike during its metasomatism, calculated by Rudnik's (1962) technique

Rock component	wt. %						Migration of substance							
	Analytical data			Reduced to 100%			Mass of component in 1000 cm <sup>3</sup> , g			Absolute difference, g		Mass difference between the samples over the mass of component in 1000 cm <sup>3</sup> of granite, %		
	VP-4	VP-17	VP-37	VP-4	VP-17	VP-37	VP-4	VP-17	VP-37	VP-17–VP-4	VP-37–VP-4	VP-17–VP-4	VP-37–VP-4	
SiO <sub>2</sub>	73.50	50.90	41.20	75.76	51.08	43.14	218.28	137.40	104.18	–80.88	–114.10	–37.05	–52.27	
TiO <sub>2</sub>	0.15	0.42	0.32	0.15	0.42	0.34	0.33	0.85	0.61	0.52	0.27	154.50	81.64	
Al <sub>2</sub> O <sub>3</sub>	13.40	28.10	28.60	13.81	28.20	29.95	46.82	89.24	85.08	42.42	38.26	90.61	81.73	
Fe <sub>2</sub> O <sub>3</sub>	1.62	8.08	4.57	1.67	8.11	4.79	3.62	16.39	8.68	12.77	5.07	353.35	140.19	
MnO	0.04	0.01	0.20	0.05	0.01	0.21	0.11	0.01	0.43	–0.10	0.32	–88.02	287.03	
MgO	0.49	0.95	0.95	0.51	0.95	0.99	2.17	3.82	3.58	1.65	1.41	76.22	65.08	
CaO	1.21	0.18	6.88	1.24	0.18	7.21	3.84	0.52	18.63	–3.32	14.79	–86.45	385.30	
Na <sub>2</sub> O	2.63	0.24	0.13	2.71	0.24	0.14	15.12	1.25	0.64	–13.86	–14.48	–91.71	–95.79	
K <sub>2</sub> O	3.58	8.22	9.87	3.69	8.25	10.33	23.20	48.41	54.45	25.22	31.26	108.70	134.75	
P <sub>2</sub> O <sub>5</sub>	0.16	0.10	0.29	0.16	0.10	0.30	0.40	0.23	0.62	–0.17	0.22	–43.19	54.33	
SO <sub>2</sub>	0.24	2.45	2.49	0.25	2.46	2.61	0.67	6.20	5.90	5.53	5.23	827.87	783.39	
Σ	97.02	99.65	95.50	100.00	100.00	100.00	314.55	304.32	282.80	–10.23	–31.75	–3.25	–10.09	
D <sub>vol</sub> , g/cm <sup>3</sup>	2.87	2.68	2.41	–	–	–	–	–	–	–	–	–	–	
D <sub>sp</sub>	2.90	2.75	2.68	–	–	–	–	–	–	–	–	–	–	
P, %	1.04	2.58	10.25	–	–	–	–	–	–	–	–	–	–	

Note. Rocks from the Vtoropavlovskaya dike: VP-4, granite, VP-17, quartz–muscovite metasomatite, VP-37, muscovite metasomatite.  $D_{vol}$ , volume mass of rock;  $d_{sp}$ , rock density; P, rock porosity. Analysis for rock-forming components was carried out by approximate quantitative atomic-emission spectroscopy (Russian Geological Research Institute, St. Petersburg, analysts V.A. Shishlov and V.L. Kudryashov).

Analysis of the HFSE patterns of rocks from the Andreevskaya and Vtoropavlovskaya dikes (Fig. 6*d, e*) confirms the above-considered regularities. Comparison of the composition of rocks from all dikes (Fig. 6*f*) shows that granites and quartz–muscovite metasomatites have similar HFSE patterns, except for Zr and Hf, and that muscovite metasomatites are enriched in most of HFSE.

Analysis of the LILE patterns (the LILE contents are given in supplementary materials ([http://sibran.ru/journals/Stepanov\\_et\\_al\\_Supplementary.docx](http://sibran.ru/journals/Stepanov_et_al_Supplementary.docx))) revealed two crucial regularities: a decrease in Sr contents from granites to quartz–muscovite and muscovite metasomatites (Fig. 7*b, c*) and higher W contents in metasomatites. Quartz–muscovite metasomatites are slightly enriched in W, whereas muscovite metasomatites contain three to four times more tungsten than granites (Fig. 7*c*). Analysis of different rocks for LILE showed that metasomatites are poorer in Li than granites (Fig. 7*d*).

Correlation analysis of the contents of trace elements in the studied rocks revealed As, Sb, Tl, Pb, Bi, In, Ag, Ga, Cu, Zn, Cd, Se, Te, Co, and Ni in the gold ore assemblage (Fig. 8). In addition, we examined the contents of W and Ge. The contents of the above elements, except for Au and Te, vary insignificantly in unaltered granites (Fig. 8*a*) because of the weak ore-forming processes in these rocks. Quartz–muscovite metasomatites have higher contents of all trace

elements of the gold ore assemblage, except for Ge (Fig. 8*b*), than granites. The highest contents have been established for As, Sb, Pb, Bi, Ag, Cu, Co, and Ni. Muscovite metasomatites are enriched in W, As, Sb, Co, and Ni relative to granites (Fig. 8*c*). The contents of the above elements are given in supplementary materials ([http://sibran.ru/journals/Stepanov\\_et\\_al\\_Supplementary.docx](http://sibran.ru/journals/Stepanov_et_al_Supplementary.docx)).

**Accessory minerals of quartz–muscovite and muscovite metasomatites.** The study of polished sections of different metasomatites has revealed numerous newly formed minerals concentrating trace elements.

Monazite-(Ce) is among the commonest REE-concentrating minerals. It is widespread in muscovite metasomatites (Fig. 9*a–c*) and scarcer in quartz–muscovite ones (Fig. 9*d*). Monazite occurs as fine intricately faceted individual grains and is found together with pyrite, apatite, and zircon predominantly in mica. The contents of La, Ce, and other REE in the mineral vary significantly (Table 2). Newly formed zircon is widespread as well-developed long-prismatic crystals, often with a distinct growth zoning, in quartz–muscovite metasomatites (Fig. 9*d, e*) but scarcer in muscovite metasomatites. Relict zircons of granites are often replaced during the rock metasomatism. For example, quartz–muscovite metasomatites from the Andreevskaya dike contain both zircon replaced by an intricate fine-crystalline aggregate (supposedly, thorianite) and relict zircon

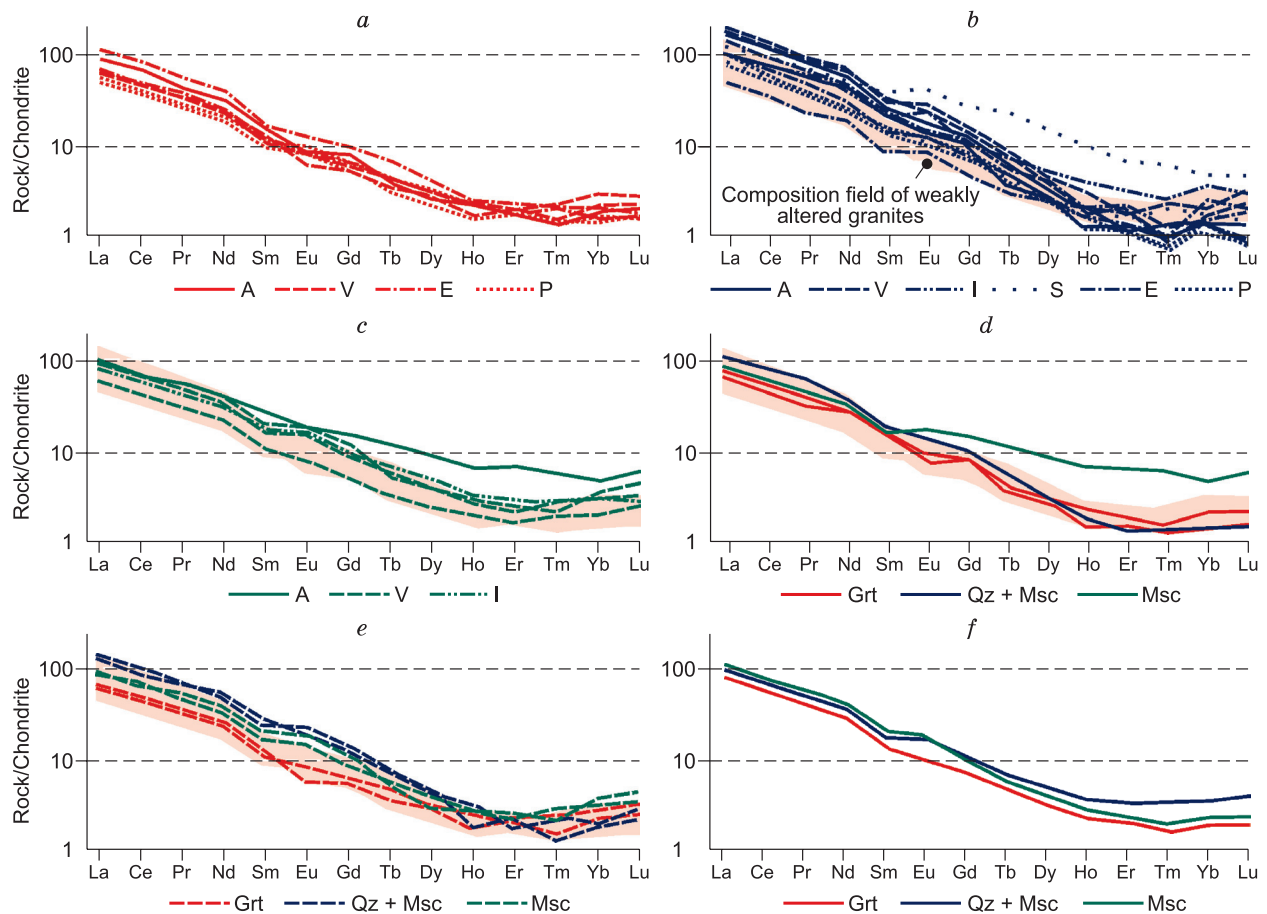


**Fig. 5.** REE patterns of granites (*a*) and apogranite metasomatites (*b*, *c*) from the Andreevskaya (A), Vtoropavlovskaya (V), Elizavetinskaya (E), Pervopavlovskaya (P), Il'inskaya (I), and Sevast'yanovskaya (S) dikes and of all rocks from the Andreevskaya (*d*) and Vtoropavlovskaya (*e*) dikes and average REE patterns for all dikes (*f*). Grt, granites, Qz + Msc, quartz–muscovite metasomatites (*b*), Msc, muscovite metasomatites (*c*). Here and in Figs. 6–8, the REE patterns are chondrite C1-normalized (McDonough and Sun, 1995). Pink field (*b*–*e*) marks the compositions of weakly altered granites.

(Fig. 9f). The main impurity in the zircon is Hf. Its content reaches 1.03 wt.% in the unaltered zircon (Table 2). Newly formed accessory apatite is also abundant. It occurs as small, most likely, pinacoidal crystals of varying size (on average, 50–70  $\mu\text{m}$ ). Most of the analyzed apatite samples contain on average 3.7 wt.% F.

Uraninite is the most widespread U–Th mineral in muscovite metasomatites. It was identified in the rock samples from the Vtoropavlovskaya and Andreevskaya dikes. Uraninite is often found as grain chains together with pyrite in muscovite aggregate (Fig. 10a, b, d). More seldom it forms rims over large pyrite metacrystals (Fig. 10c). The mineral contains up to 2.20 wt.% Th, 3.12–8.54 wt.% Pb, and 1–3 wt.% Fe (Table 3). Thorianite forms intricate metasomatic aggregates replacing zircon (Fig. 10e) or occurs as euhedral inclusions smaller than 10  $\mu\text{m}$  in pyrite (Fig. 10f). The performed chemical analyses show the presence of all minerals of the isomorphous series uraninite–thorianite in muscovite metasomatites.

Minerals concentrating Sn, namely, cassiterite, ferrokassiterite, and stannite, were detected only as inclusions in pyrite metacrystals from muscovite metasomatites (Fig. 11; Table 4). Tungsten is accumulated in krasnogorite, W-containing rutile, and scheelite present mostly in muscovite metasomatites. Scheelite often occurs as euhedral crystals measuring fractions of mm to a few cm in muscovite metasomatites from the Il'inskaya, Sevast'yanovskaya, and Vtoropavlovskaya dikes and is scarcer in similar metasomatites from the Andreevskaya dike. Seldom, scheelite crystals reach a few cm in size.

Pyrite is the only sulfide ore mineral widespread in muscovite metasomatites; seldom, galena is also present (Fig. 12a). Quartz–muscovite metasomatites often contain complex intergrowths of pyrite, galena, fahlores (mostly tennantite), chalcocopyrite, and other minerals (Fig. 12b–d). A crucial morphologic feature of this pyrite is a predominance of pentagonal dodecahedral crystals in muscovite metasomatites and of cubic crystals with an oscillatory-



**Table 2.** Composition of monazite, zircon, apatite, and thorite from quartz–muscovite and muscovite metasomatites, wt.%

Run	Sample	SiO <sub>2</sub>	P <sub>2</sub> O <sub>5</sub>	CaO	ZrO <sub>2</sub>	HfO <sub>2</sub>	La <sub>2</sub> O <sub>3</sub>	Ce <sub>2</sub> O <sub>3</sub>	Pr <sub>2</sub> O <sub>3</sub>	Nd <sub>2</sub> O <sub>3</sub>	Sm <sub>2</sub> O <sub>3</sub>	Gd <sub>2</sub> O <sub>3</sub>	F	ThO <sub>2</sub>	Σ	Formula
1	VP-37	–	30.12	–	–	–	17.49	33.70	3.75	11.05	2.15	1.19	–	–	100.02	(Ce <sub>0.48</sub> La <sub>0.25</sub> Nd <sub>0.16</sub> Pr <sub>0.05</sub> Sm <sub>0.03</sub> Gd <sub>0.02</sub> Dy <sub>0.01</sub> ) <sub>0.99</sub> PO <sub>4</sub>
2	VP-37	–	41.94	54.94	–	–	–	–	–	–	–	–	3.15	–	100.02	Ca <sub>4.99</sub> (P <sub>1.00</sub> O <sub>4</sub> ) <sub>3</sub> F <sub>0.84</sub>
3	VP-37	–	41.87	54.82	–	–	–	–	–	–	–	–	3.22	–	99.92	Ca <sub>5.06</sub> (P <sub>1.02</sub> O <sub>4</sub> ) <sub>3</sub> F <sub>0.88</sub>
4	VP-35	–	29.98	–	–	–	21.51	36.18	3.64	8.78	–	–	–	–	100.09	(Ce <sub>0.52</sub> La <sub>0.31</sub> Nd <sub>0.12</sub> Pr <sub>0.05</sub> ) <sub>1.00</sub> PO <sub>4</sub>
5	VP-35	–	30.05	2.13	–	–	13.58	32.18	2.72	10.60	–	–	–	8.49	99.74	(Ce <sub>0.46</sub> La <sub>0.19</sub> Nd <sub>0.16</sub> Pr <sub>0.04</sub> ) <sub>1.00</sub> PO <sub>4</sub>
6	DE-1	–	30.55	–	–	–	17.30	34.34	3.73	11.23	1.53	0.93	–	–	100.00	(Ce <sub>0.50</sub> La <sub>0.25</sub> Nd <sub>0.16</sub> Pr <sub>0.05</sub> Sm <sub>0.02</sub> Gd <sub>0.01</sub> ) <sub>1.00</sub> PO <sub>4</sub>
7	DE-1	32.61	–	–	65.90	1.61	–	–	–	–	–	–	–	–	100.12	Zr <sub>0.99</sub> Hf <sub>0.01</sub> SiO <sub>4</sub>
8	DE-1	–	41.51	54.44	–	–	–	–	–	–	–	–	3.36	–	99.32	Ca <sub>5.00</sub> (P <sub>1.00</sub> O <sub>4</sub> ) <sub>3</sub> F <sub>0.91</sub>
9	DE-1	32.69	–	–	66.45	0.84	–	–	–	–	–	–	–	–	99.98	Zr <sub>0.99</sub> Hf <sub>0.01</sub> SiO <sub>4</sub>
10	DE-1	32.51	–	–	66.85	0.51	–	–	–	–	–	–	–	–	99.87	Zr <sub>0.99</sub> SiO <sub>4</sub>
11	DE-1	32.09	–	–	66.40	1.54	–	–	–	–	–	–	–	–	100.03	Zr <sub>0.99</sub> Hf <sub>0.01</sub> SiO <sub>4</sub>
12	DE-1	–	41.71	55.01	–	–	–	–	–	–	–	–	3.12	–	99.84	Ca <sub>5.01</sub> (P <sub>1.00</sub> O <sub>4</sub> ) <sub>3</sub> F <sub>0.84</sub>
13	DA-11	27.69	–	0.38	53.94	1.16	–	–	–	–	–	–	–	5.38	88.54	–
14	DA-11	13.31	–	2.49	14.33	–	–	–	–	–	–	–	–	45.55	75.68	–
15	DA-11	25.14	–	1.34	47.59	2.61	–	–	–	–	–	–	–	2.45	81.85	–

Note. Contents of components: 1, Dy<sub>2</sub>O<sub>3</sub> = 0.57 wt.%; 15, UO<sub>2</sub> = 2.72 wt.%. 1, 4, 5, 6, monazite; 2, 3, 8, 12, apatite; 7, 9–11, zircon; 13–15, minerals of the isomorphous series zircon–thorite. Formulae were calculated per four oxygen atoms. The composition of minerals was determined with a JEOL-JSM6390LV scanning electron microscope equipped with a Link Pentafet EMF spectrometer (Institute of Geology and Geochemistry, Yekaterinburg, analyst E.S. Shagalov).

**Table 3.** Composition of Th–U minerals from quartz–muscovite and muscovite metasomatites, wt.%

Run	Sample	SiO <sub>2</sub>	CaO	TiO <sub>2</sub>	FeO	ZrO <sub>2</sub>	PbO	ThO <sub>2</sub>	UO <sub>2</sub>	Σ	Formula
1	DA-31	–	1.36	–	0.86	–	4.06	1.80	90.83	98.91	(U <sub>0.91</sub> Ca <sub>0.07</sub> Pb <sub>0.05</sub> Fe <sub>0.03</sub> Th <sub>0.02</sub> ) <sub>1.07</sub> O <sub>2</sub>
2	DA-11	–	1.35	2.73	0.90	15.58	–	–	78.79	99.35	(U <sub>0.62</sub> Zr <sub>0.27</sub> Ti <sub>0.07</sub> Ca <sub>0.05</sub> Fe <sub>0.03</sub> ) <sub>1.04</sub> O <sub>2</sub>
3	DA-11	–	2.99	0.00	0.68	5.16	–	–	76.92	90.51	(U <sub>0.74</sub> Ca <sub>0.14</sub> Zr <sub>0.11</sub> Fe <sub>0.02</sub> W <sub>0.05</sub> ) <sub>1.06</sub> O <sub>2</sub>
4	DA-31	–	1.53	1.18	2.15	2.72	–	–	64.57	72.15	(U <sub>0.79</sub> Fe <sub>0.10</sub> Ca <sub>0.09</sub> Zr <sub>0.07</sub> Ti <sub>0.05</sub> ) <sub>1.09</sub> O <sub>2</sub>
5	VP-37	–	–	–	–	–	9.20	2.50	69.21	80.92	(U <sub>0.89</sub> Pb <sub>0.14</sub> Th <sub>0.03</sub> ) <sub>1.07</sub> O <sub>2</sub>
6	VP-1	8.67	1.05	–	0.81	4.36	3.36	41.18	18.47	77.90	–
7	VP-1	4.32	0.62	–	0.80	4.01	27.73	25.47	12.76	75.70	–
8	DA-21	6.35	–	–	–	–	–	44.08	31.59	82.03	–

Note. 3, W<sub>2</sub>O<sub>3</sub> = 8.76 wt.%. 1–5, uraninite, formulae were calculated per two oxygen atoms; 6–8, a mixture of minerals of the isomorphous series thoria–uraninite and other silicates. The composition of minerals was determined with a JEOL-JSM6390LV scanning electron microscope equipped with a Link Pentafet EMF spectrometer (Institute of Geology and Geochemistry, Yekaterinburg, analyst E.S. Shagalov).

combination striation (due to their transition to a pentagonal dodecahedron) in quartz–muscovite metasomatites. Some pyrite metacrystals from quartz–muscovite metasomatites, especially from the near-selvage zones of sulfide–quartz veins, contain small inclusions of native gold with Ag impurity (Fig. 12d; Table 5).

Thus, we have established major newly formed accessory minerals in the studied rocks: zircon, rutile, pyrite, fahlores, galena, and chalcopyrite in quartz–muscovite metasomatites and zircon, monazite, fluorapatite, pyrite, and uraninite in muscovite metasomatites. The results of the performed stud-

ies show the presence of different mineral assemblages in quartz–muscovite and muscovite metasomatites.

## DISCUSSION

The established sequence of granite replacement processes in dikes in the northern part of the Berezovskoe ore field is similar to the sequence of metasomatic transformations of dike rocks in its southern part (Borodaevskaya, 1944; Borodaevskii and Borodaevskaya, 1947; Popov, 1970), granites

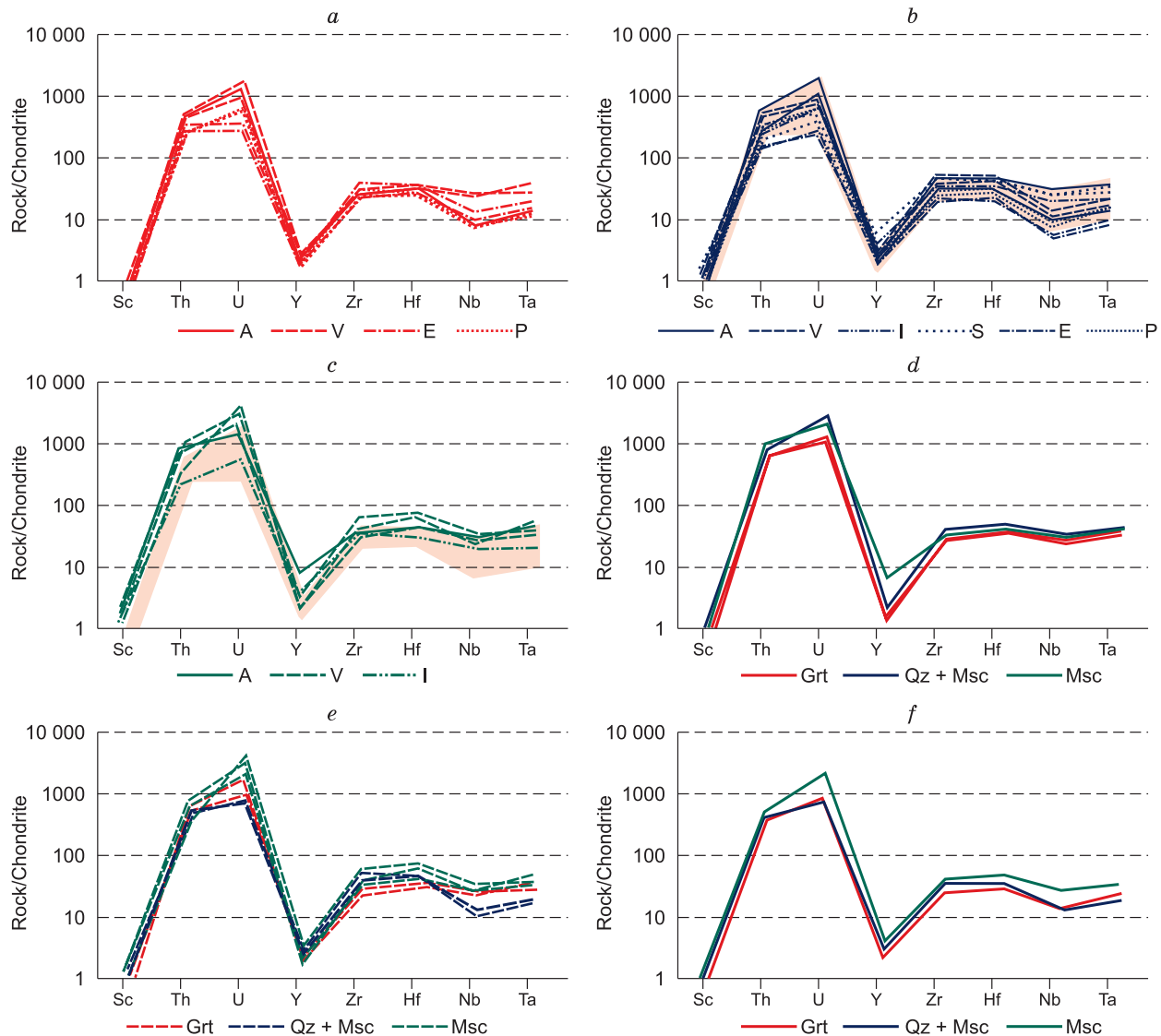


**Fig. 6.** HFSE patterns of granites (a) and apogranite metasomatites (b, c) from dikes, average HFSE contents in different rocks of the Andreevskaya (d) and Vtoropavlovskaya (e) dikes, and average HFSE contents in rocks from all dikes (f). Light pink field marks the compositions of granites. Other designations follow Fig. 5.

of the Shartash intrusive massif (Grabezhev, 1970), and rocks of beresite–listwänite association in general (Sazonov and Borodaevskii, 1980). Apogranite metasomatites developed within the Berezovskoe gold deposit are diverse (Borodaevskaya, 1944; Borodaevskii and Borodaevskaya, 1947). Near-vein quartz–muscovite and near-fracture muscovite metasomatites prevail in the northern part of the ore field. Note that the term “beresites” is not quite appropriate for these metasomatic rocks, because they are composed predominantly of muscovite and lack sericite (Plyushchev et al., 2012).

The proximal spatial localization of two types of metasomatites (Fig. 4) points to their formation during the same process but at its different stages. As in the southern part of the Berezovskoe ore field, the studied muscovite metasoma-

titites are similar to coarse-foliated mica beresites formed at the greisen stage (Borodaevskii and Borodaevskaya, 1947). Quartz–muscovite metasomatites are similar to fine-grained mica–quartz beresites formed at the lower-temperature stage following the greisen one (Borodaevskii and Borodaevskaya, 1947). Successive replacement of muscovite metasomatites by quartz–muscovite ones was extremely rare.

The partial removal of  $\text{SiO}_2$ , the total loss of  $\text{Na}_2\text{O}$ , and the input of  $\text{K}_2\text{O}$  and  $\text{Al}_2\text{O}_3$  are the main processes reflecting a change in the chemical composition of granites during their metasomatic transformation, which was also shown in the earlier studies (Borodaevskaya, 1944; Borodaevskii and Borodaevskaya, 1947; Grabezhev, 1970; Popov, 1971). The calculated loss of substance during metasomatism is 3.25 wt.% for quartz–muscovite metasomatites and 10.9 wt.%

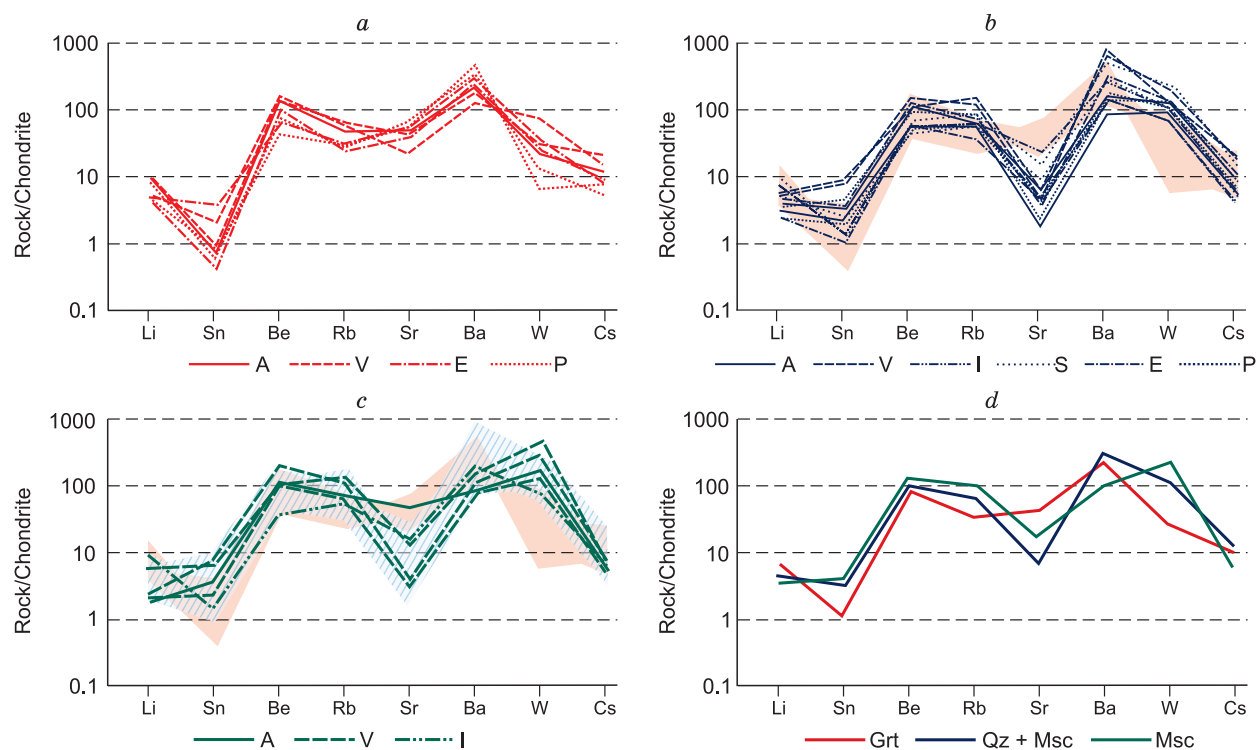
**Table 4.** Composition of W- and Sn-concentrating minerals from quartz–muscovite and muscovite metasomatites, wt.%

Run	Sample	O	S	Ti	Fe	Cu	Zn	Sn	Mo	W	Ca	Σ
1	DE-1.2	21.10	–	–	–	–	–	78.20	–	–	–	99.30
2	VP-54	–	29.53	–	7.14	29.04	6.63	27.46	–	–	–	99.80
3	VP-54	–	29.36	–	5.34	28.61	9.02	27.35	–	–	–	99.68
4	VP-54	21.12	–	–	–	–	–	78.62	–	–	–	99.74
5	DA-31	21.87	–	2.86	–	–	–	–	–	74.87	–	99.60
6	SD-4	38.23	–	54.43	1.64	–	–	–	–	4.90	–	99.20
7	SD-4	38.95	–	58.38	0.23	–	–	–	–	1.20	–	98.76
8	ID-32	21.90	–	–	–	–	–	–	–	64.04	13.55	99.49
9	ID-32	22.14	–	–	–	–	–	–	0.02	63.52	13.75	99.43
10	ID-32	21.94	–	–	–	–	–	–	–	63.98	13.63	99.55

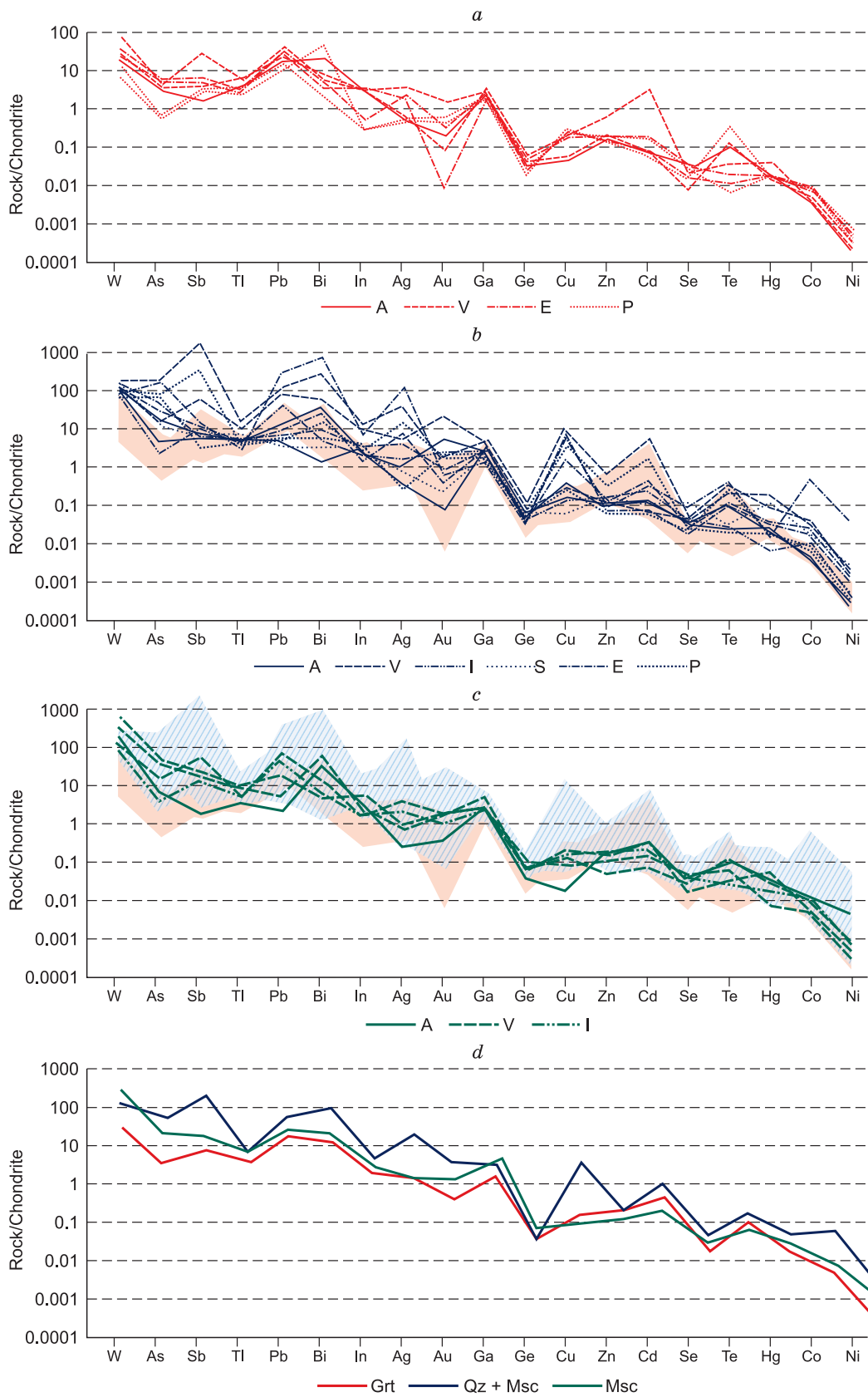
  

Empirical formulae	
1	Cassiterite $\text{Sn}_{0.99}\text{O}_2$
2	Ferrokesterite $\text{Cu}_{1.98}\text{Fe}_{0.56}\text{Zn}_{0.44}\text{SnS}_4$
3	Kesterite $\text{Cu}_{1.97}\text{Zn}_{0.60}\text{Fe}_{0.42}\text{SnS}_4$
4	Cassiterite $\text{Sn}_{1.01}\text{O}_2$
5	Krasnogorite $\text{W}_{0.89}\text{Ti}_{0.13}\text{O}_2$
6	W-containing rutile $\text{Ti}_{0.95}\text{Fe}_{0.02}\text{W}_{0.02}\text{O}_2$
7	W-containing rutile $\text{Ti}_{0.95}\text{W}_{0.01}\text{O}_2$
8	Scheelite $\text{CaWO}_4$
9	Scheelite $\text{CaWO}_4$
10	Scheelite $\text{CaWO}_4$

Note. 1, 4, 5, 6, 7, formulae were calculated per two oxygen atoms; 2, 3, per eight oxygen atoms; 8, 9, per four oxygen atoms. The composition of minerals was determined with a JEOL-JSM6390LV scanning electron microscope equipped with a Link Pentafet EMF spectrometer (Institute of Geology and Geochemistry, Yekaterinburg, analyst E.S. Shagalov).



**Fig. 7.** LILE patterns of granites (a) and apogranite metasomatites (b, c) and average LILE contents in rocks from all dikes (d). Hatched field (c) marks the compositions of quartz–muscovite metasomatites. Other designations follow Fig. 5.



**Fig. 8.** Spidergrams of typical elements of gold mineral assemblage of granites (*a*) and apogranite metasomatites (*b*, *c*) and their average contents in different rocks from all dikes (*d*). Other designations follow Figs. 5 and 7.

**Table 5.** Composition of sulfide minerals (1–14) and gold (15) from quartz–muscovite metasomatites, wt.%

Run	Sample	S	Fe	Cu	Zn	As	Sb	Ag	Pb	Au	Σ	Formula
1	VP-17	53.15	46.10	–	–	0.81	–	–	–	–	100.06	Fe <sub>1.00</sub> As <sub>0.01</sub> S <sub>2.00</sub>
2	VP-17	53.30	46.14	–	–	–	–	–	–	–	99.46	Fe <sub>0.99</sub> S <sub>2.00</sub>
3	VP-17	13.46	0.18	0.44	–	–	–	–	85.22	–	99.30	Pb <sub>0.98</sub> Cu <sub>0.02</sub> Fe <sub>0.01</sub> S <sub>1.00</sub>
4	SD-2	14.09	0.21	0.39	–	–	–	1.23	83.76	–	99.68	Pb <sub>0.93</sub> Ag <sub>0.03</sub> Cu <sub>0.02</sub> S <sub>1.02</sub>
5	SD-2	27.44	4.98	41.53	2.76	16.22	5.51	0.53	–	–	98.97	(Cu <sub>9.94</sub> Ag <sub>0.07</sub> ) <sub>10.01</sub> (Zn <sub>0.64</sub> Fe <sub>1.36</sub> ) <sub>2.00</sub> (As <sub>3.29</sub> Sb <sub>0.69</sub> ) <sub>3.98</sub> S <sub>13.01</sub>
6	SD-2	53.72	46.83	0.05	–	0.12	–	–	–	–	100.72	Fe <sub>1.00</sub> S <sub>2.00</sub>
7	ID-7	53.39	46.54	–	–	–	–	–	–	–	99.99	Fe <sub>1.00</sub> S <sub>2.00</sub>
8	ID-7	27.56	2.36	42.57	5.24	15.83	6.12	0.29	–	–	99.97	(Cu <sub>10.14</sub> Ag <sub>0.04</sub> ) <sub>10.18</sub> (Zn <sub>1.21</sub> Fe <sub>0.64</sub> ) <sub>1.85</sub> (As <sub>3.20</sub> Sb <sub>0.76</sub> ) <sub>3.96</sub> S <sub>13.01</sub>
9	ID-7	13.27	0.29	–	–	–	–	0.40	86.49	–	100.45	Pb <sub>0.99</sub> Ag <sub>0.01</sub> Fe <sub>0.01</sub> S <sub>0.99</sub>
10	DE-8	13.81	0.25	0.34	–	–	–	1.93	82.81	–	99.14	Pb <sub>0.93</sub> Ag <sub>0.04</sub> Cu <sub>0.01</sub> S <sub>1.00</sub>
11	DE-8	53.88	45.95	–	–	0.56	–	–	–	–	100.45	FeAs <sub>0.01</sub> S <sub>2</sub>
12	DE-8	53.96	45.71	–	–	0.45	–	–	–	–	100.18	FeAs <sub>0.01</sub> S <sub>2</sub>
13	DE-8	28.17	5.22	44.93	1.15	19.36	1.27	–	–	–	100.10	Cu <sub>10.43</sub> (Fe <sub>1.38</sub> Zn <sub>0.26</sub> ) <sub>1.64</sub> (As <sub>3.81</sub> Sb <sub>0.15</sub> ) <sub>3.97</sub> S <sub>12.96</sub>
14	DE-8	35.71	29.98	34.11	–	–	–	–	–	–	99.80	FeAs <sub>0.01</sub> S <sub>2</sub>
15	DE-8	–	–	–	–	–	–	9.06	–	90.89	99.95	Au <sub>0.85</sub> Ag <sub>0.15</sub>

Note. 2, 7, 11, 12, Co = 0.02 wt.%, 7, 11, Ni = 0.04 wt.%. 1, 2, 6, 7, 11, 12 (pyrite), formulae were calculated per two sulfur atoms, 3, 4, 9, 10 (galena), per two oxygen atoms, 5, 8, 13 (fahlore), per 29 oxygen atoms, 14 (chalcopyrite), per four oxygen atoms. The composition of minerals was determined with a JEOL-JSM6390LV scanning electron microscope equipped with a Link Pentafet EMF spectrometer (Institute of Geology and Geochemistry, Yekaterinburg, analyst E.S. Shagalov).

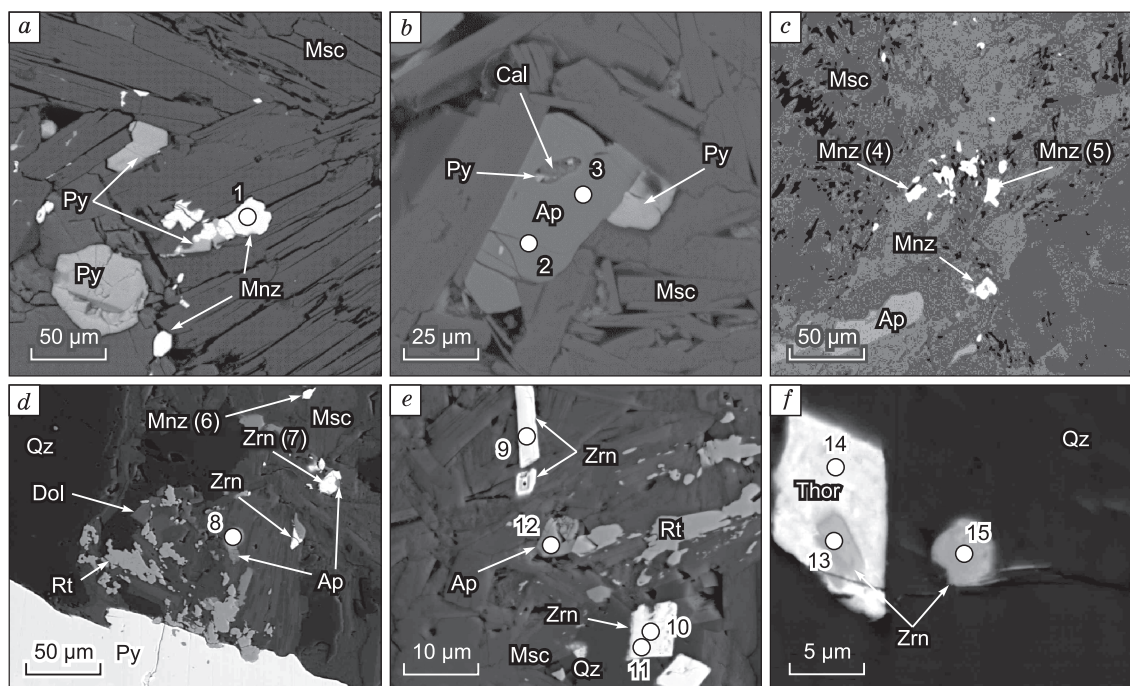


**Fig. 9.** Newly formed accessory minerals in muscovite (a–c) and quartz–muscovite (d–f) metasomatites developed after granites of the Vtoropavlovskaya (a, b), Andreevskaya (c, f), and Elizavetinskaya (d, e) dikes. Numerals and encircled numerals mark the points of analyses considered in Table 2. Msc, muscovite, Qz, quartz, Py, pyrite, Zrn, zircon, Ap, apatite, Rt, rutile, Mnz, monazite-(Ce), Dol, Fe-containing dolomite, Cal, calcite, Thor, thorianite.

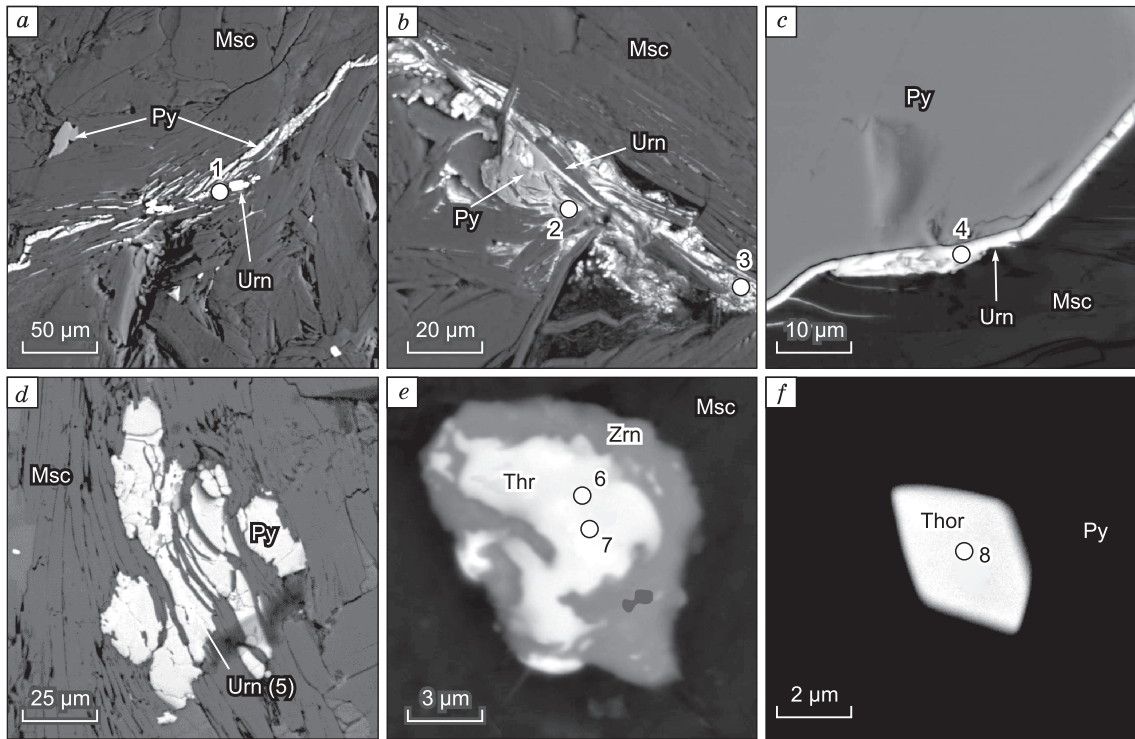


**Fig. 10.** Newly formed Th–U minerals in quartz–muscovite and muscovite metasomatites developed after granites of the Andreevskaya (*a, b, c*, *f*) and Vtoropavlovskaya (*d, e*) dikes. Numerals and encircled numerals mark the points of analyses considered in Table 3. Urn, uraninite. Other designations follow Fig. 9.

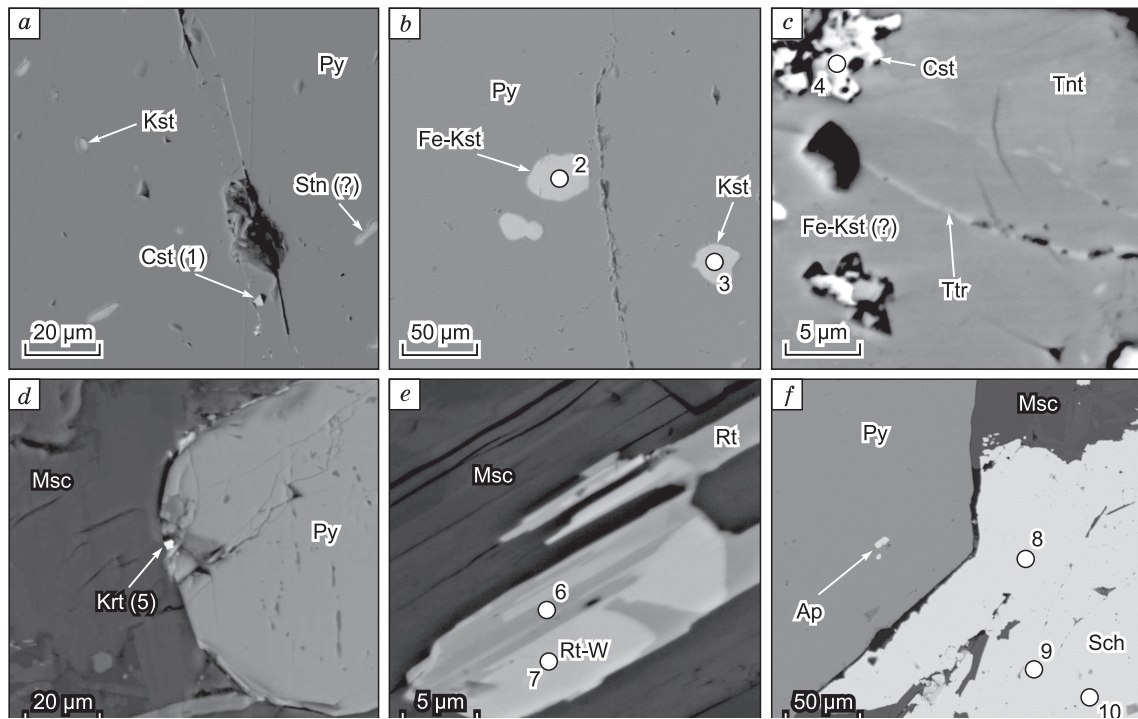


**Fig. 11.** Minerals concentrating Sn (*a–c*) and W (*d–f*) as inclusions in sulfides or as individual grains in muscovite metasomatites from the Elizavetinskaya (*a*), Vtoropavlovskaya (*b, c*), Andreevskaya (*d*), Sevast’yanovskaya (*e*), and Il’inskaya (*f*) dikes. Numerals and encircled numerals mark the points of analyses considered in Table 4. Cst, cassiterite, Stn(?), mineral similar in composition to stannite, Kst, kesterite, Fe–Kst, ferrokesterite, Tnt, tennantite, Ttr, tetrahedrite, Krt, krasnogorite(?), Rt–W, W-containing rutile, Rt, rutile, Ap, apatite, Sch, scheelite. Other designations follow Fig. 9.

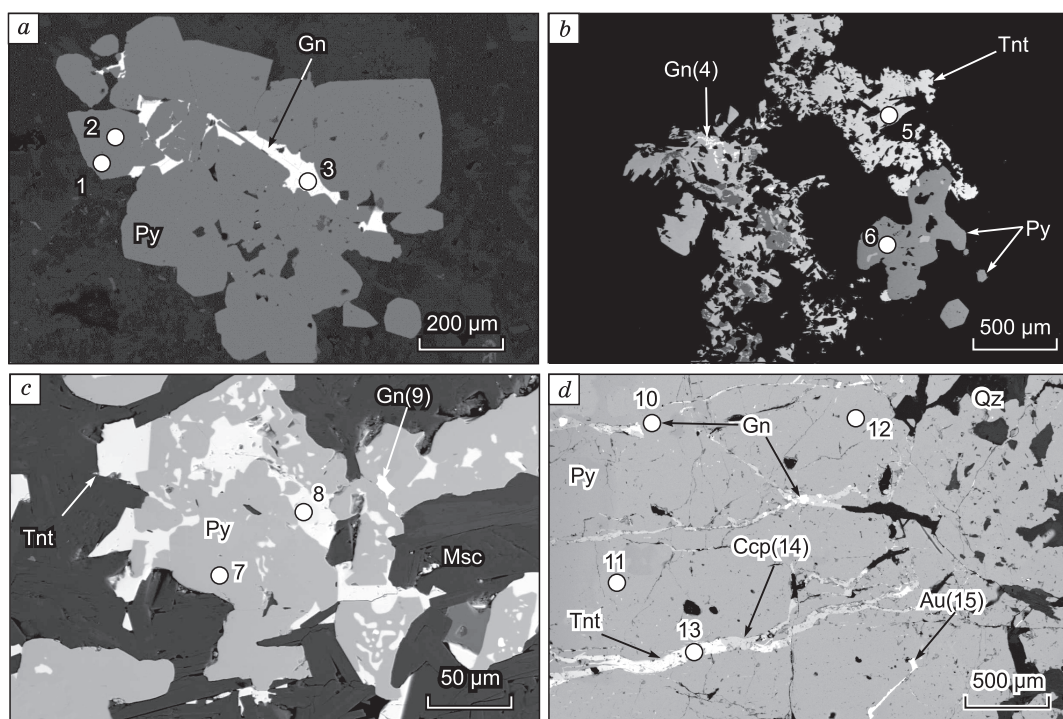


**Fig. 12.** Aggregates of sulfide minerals from apogranite metasomatites from the Vtoropavlovskaya (a), Sevast'yanovskaya (b, c), and Elizavetinskaya (d) dikes. Numerals and encircled numerals mark the points of analyses considered in Table 5. Gn, galena, Ccp, chalcocopyrite, Au, native gold. Other designations follow Figs. 9, 11.

for muscovite metasomatites from the Vtoropavlovskaya dike. Most of the lost substance is  $\text{SiO}_2$ , which is spent mainly for the formation of quartz in sulfide–quartz veins (Popov, 1971). Muscovite metasomatites formed before sulfide–quartz veins, and quartz–muscovite metasomatites, synchronously with them. Thus, muscovite metasomatites form during the removal of some components ( $\text{SiO}_2$ ,  $\text{Na}_2\text{O}$ ) into a hydrothermal system, and quartz–muscovite metasomatites (like sulfide–quartz veins), during the input of substance.

The studied dike granite–porphyry from the Berezovskoe ore field is similar in trace-element patterns to granites of the Verkhnyaya Iset' massif (Fershtater, 2013). Even weakly altered dike granites bear disseminated sulfide minerals; as a result, the Au content in these granites is an order of magnitude higher than its standard content in crustal rocks (Pitcairn, 2011).

The first results of a geochemical analysis of metasomatites for 51 elements and their trace-element patterns indicate that the replacement of granites by quartz–muscovite and muscovite metasomatites is accompanied by an increase in the contents of many trace elements, first of all, Sc, Th, U, Zr, Hf, Nb, Ta, REE, Cu, Ga, Ge, As, Se, In, Sb, Tl, Pb, Bi, W, Sn, Rb, Ag, and Au. Correlation and factor analyses showed two geochemical associations of the above elements (Fig. 13). One association includes W, Sc, Zr, Hf, Ga, REE, U, Th, Ta, and Nb, accumulated during the formation of muscovite metasomatites. The other comprises Cu, Pb, Bi,

As, Sb, Co, Ni, Ba, In, Cd, Mo, Te, Ag, and Au, intimately correlated with gold and accumulated mainly during the formation of near-vein quartz–muscovite metasomatites. These associations supplement the known characteristics of different metasomatites. The elements of the former association are typical of greisenization, and the elements of the latter are specific to gold deposits of intrusive complexes (Schreiber et al., 1990; Sillitoe and Thompson, 1998; Hart and Goldfarb, 2005).

The accumulation of HFSE and REE, almost immobile during metamorphic and hydrothermal processes (Pearce and Cann, 1971; Floyd and Winchester, 1975; MacLean and Barrett, 1993; Sklyarov et al., 2001), is confirmed by results of mineralogical studies. We have established a decrease in  $(\text{La}/\text{Lu})_N$  during the replacement of granites by quartz–muscovite metasomatites, which is due to the abundance of newly formed zircon (concentrating HREE) in the latter. Formation of muscovite metasomatites is, on the contrary, accompanied by an increase in  $(\text{La}/\text{Lu})_N$ . This phenomenon is explained by scarce newly formed zircon and abundant newly formed monazite (earlier, monazites were found by Pribavkin (2002) only in pegmatites of the Shartash massif) and fluorapatite. The increase in Zr and Hf contents in all metasomatites relative to granites is due to the formation of minerals of the isomorphous series zircon–coffinite–thorite.

Until 2018, there were no publications on radioactive-element minerals of the Berezovskoe deposit. Only an uncon-

firmed finding of torbernite in 1988 was mentioned (Sustavov, 2002). During the study of muscovite and quartz–muscovite metasomatites, we discovered thorianite and uraninite. Fine brannerite grains were found as inclusions in pyrite from sulfide–quartz veins in granite dikes of the Berezovskoe deposit (Popova et al., 2018; Shagalov et al., 2018). Minerals of the series thorite–coffinite were identified in pyrites from muscovite metasomatites (Shagalov et al., 2018). The revealed U–Th mineralization in muscovite metasomatites explains their enrichment in these elements relative to unaltered granites.

The presence of the above-mentioned newly formed accessory minerals, except for Th- and U-containing ones, was established in high-temperature apopicitic gumbites in the northern part of the Berezovskoe ore field (Spiridonov et al., 2013). Thus, the formation of minerals concentrating poorly mobile elements confirms the earlier conclusions (Rubin et al., 1993) about the possible transfer of these elements in hydrothermal systems. At the same time, the abundance of newly formed zircon, monazite, and apatite also proves the earlier established tendency of REE accumulation during the formation of medium-temperature metasomatites of the beresite–listwänite association, including metasomatites of the Berezovskoe ore field (Sazonov et al., 2006, 2009).

The LILE patterns of metasomatites are much due to the hosted accessory minerals.

Muscovite metasomatites are enriched in Sn and W, typical ore elements of greisen association. The accumulation of Sn in metasomatites is due to the abundance of mineral inclusions in the hosted pyrite metacrystals. Earlier, cassiterite (Borodaevskii and Borodaevskaya, 1947; Pavlishin et al., 1988) and kesterite (Filimonov, 1999b) were found in

the Berezovskoe deposit. In addition, more ferruginous varieties of kesterite, up to ferrokesterite and stannite, were revealed. These minerals are similar in composition to minerals of other deposits of the same geochemical type (Moore and Howie, 1984; Kołodziejczyk et al., 2016). Scheelite is the main mineral concentrating W in metasomatites. It contains few impurities, which is typical of scheelites from hydrothermal gold deposits (Ghaderi et al., 1999). Newly formed W-containing rutile found both in quartz–muscovite and muscovite metasomatites is similar to minerals revealed earlier in gumbites of the Berezovskoe ore field (Filimonov, 2000). It has less effect on the increase in W content than scheelite.

Galena, fahlores, and chalcopyrite, like pyrite, are widespread in quartz–muscovite metasomatites. Some elements, such as As, Sb, Cu, Zn, Bi, and Ag, are present in fahlores both as mineral-forming components and as impurities (Filimonov, 2009). Quartz veins, spatially and genetically associated with quartz–muscovite metasomatites, contain minerals of Bi (Chesnokov et al., 1975; Filimonov, 1999a; Pribavkin et al., 2018), Te (Filimonov, 1999a, 2000), Cd and In (Shagalov et al., 2018). These minerals in veins are responsible for the high contents of mineral-forming components in near-vein metasomatites. The association of impurity elements Co, Ni, As, Sb, Cu, Zn, Pb, Bi, Te, Cd, In, and Ag present in quartz–muscovite metasomatites is similar to the productive gold–metal assemblage of sulfide–quartz veins of the Berezovskoe deposit (Samartsev et al., 1973). In muscovite metasomatites, Co and Ni are the only elements of the gold ore assemblage that are present in high contents. They are concentrated mainly by pyrite metacrystals.

During the metasomatic transformation of granites, their Au/Ag ratio increases: from 0.10–0.25 in weakly altered granites to 2.38–3.60 in quartz–muscovite metasomatites. This regularity is well pronounced in rocks of the Andreevskaya and Vtoropavlovskaya dikes. A similar accumulation of Au relative to Ag is also observed in muscovite metasomatites, which have slightly higher contents of Au and the same or even lower contents of Ag than granites.

Analysis of the results of geochemical studies has shown two stages of a metasomatic process. The first stage was a significant removal of SiO<sub>2</sub> and accumulation of Zr, Y, REE, Be, Sn, and W, accompanied by the formation of minerals concentrating these elements. With regard to the petrographic data, this stage corresponds to the formation of muscovite metasomatites. The second (probably, lower-temperature) stage was the accumulation of Bi, Sb, Cu, Pb, Au, and Ag and formation of sulfide–quartz veins and genetically related quartz–muscovite metasomatites.

To assess the influence of the abundance of metasomatites of different types on the gold distribution in dike blocks, it is worth examining the rock sections containing gold. In the Vtoropavlovskaya dike (Fig. 14a, b), one of the blocks with quartz–muscovite and muscovite metasomatites is characterized by an extremely uneven distribution of gold,

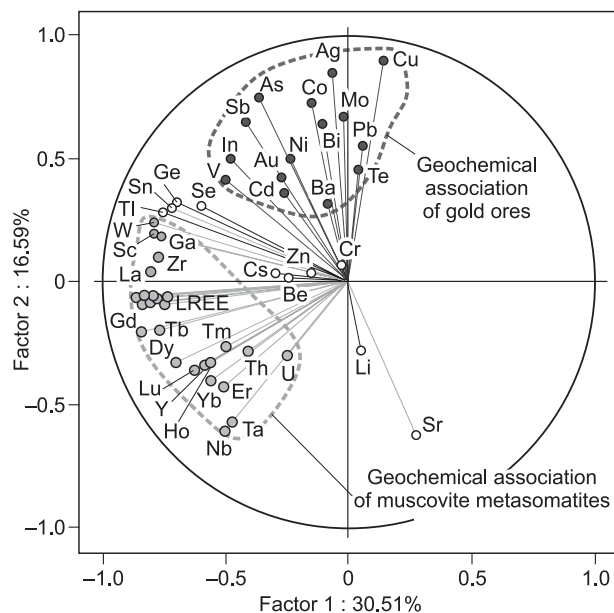
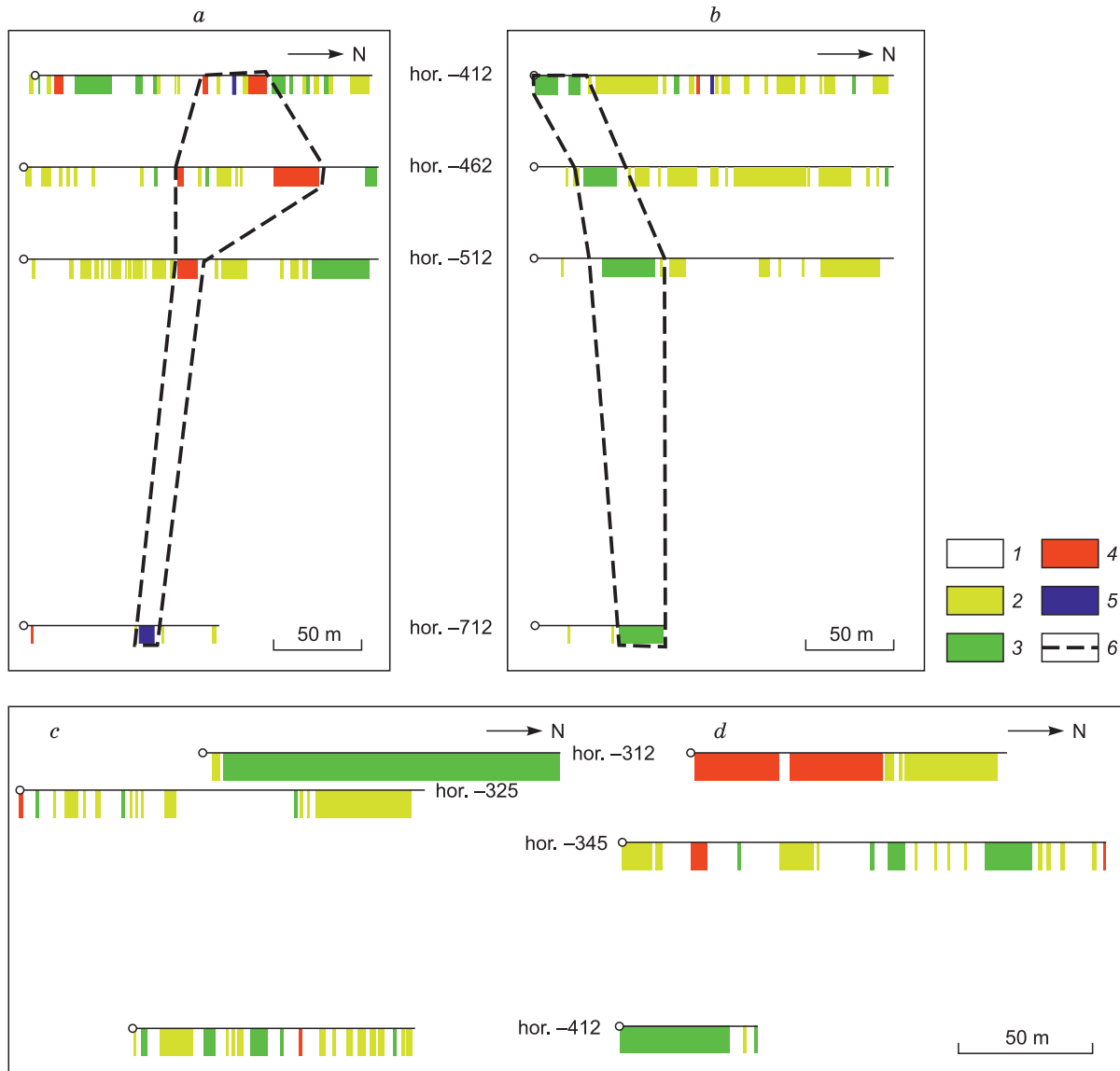


Fig. 13. Factor diagram of the element distribution (constructed from the results of factor analysis).





**Fig. 14.** Gold distribution along the western (a) and eastern (b) walls of a drift in one of the blocks of the Vtoropavlovskaya dike and along the western (c) and eastern (d) walls of a drift in the Il'inskaya dike. Gold content, ppm: 1, <1; 2, 1–3; 3, 3–5; 4, 5–10; 5, >10; 6, “ore column” contours.

which is concentrated mainly in a column-shaped zone. Apparently, the uneven distribution of gold is primarily due to the uneven distribution of sulfide–quartz veins within the block. A decrease in the number of quartz veins per unit volume of the dike body is typical of the muscovite metasomatite zones. The metasomatites, in turn, are free from sulfide minerals of the gold ore assemblage. For these reasons, the dike sites where granites are replaced by muscovite metasomatites have no commercial value. At the same time, the significant redistribution of  $\text{SiO}_2$  and ore components leads to the formation of rich column-shaped fragments of orebodies within the dikes.

A different pattern is observed in one of the blocks of the Il'inskaya dike (Fig. 14c, d), with predominant quartz–muscovite metasomatites and subordinate muscovite ones. New-

ly formed minerals of the gold ore assemblage are widespread in both of these metasomatites. Quartz veins here are evenly distributed and have steady high contents of gold, which permits us to regard large fragments of the block as gold-rich sites of commercial value.

## CONCLUSIONS

Based on the results of the performed studies, we have recognized spatially and genetically associated quartz–muscovite and muscovite metasomatites within the Berezovskoe ore field, which form at different stages of the same process. Muscovite metasomatites resulted from the removal of rock-forming components, primarily  $\text{SiO}_2$  и  $\text{Na}_2\text{O}$ , from granites.

They are similar in geochemical composition (W, Sc, Zr, Hf, Ga, REE, U, Th, Ta, and Nb) to greisens. Quartz–muscovite metasomatites formed synchronously with sulfide–quartz veins. In geochemical composition (Pb, Bi, As, Sb, Co, Ni, Ba, In, Cd, Mo, Te, Ag, and Au) they are similar to the gold–metal assemblage typical of most of intrusion-related vein gold deposits. By the examples of local dike zones, we have demonstrated that the conditions of formation of muscovite–quartz metasomatites are the most favorable for the origin of gold mineralization.

This mineralization is localized in sulfide–quartz veins and, to a lesser extent, in the near-vein quartz–muscovite metasomatites. Silica necessary for the formation of these metasomatites and quartz veins is released during the genesis of muscovite metasomatites. Based on the research results, we have described a single hydrothermal-metasomatic system. Within this system, greisen-like high-temperature metasomatites form in the course of the removal of components, and low-temperature metasomatites, similar in mineral composition to beresites with gold ore signatures, appear during the input of elements.

The commercial gold reserves are revealed in the areas with the maximum spread of quartz–muscovite metasomatites. Muscovite metasomatites formed during the removal of rock-forming components affect negatively the distribution of sulfide–quartz veins within metasomatically transformed granite dikes. This explains the extremely uneven distribution of gold, with the formation of column-shaped orebodies, which significantly complicates the correct evaluation of gold reserves during geological exploration.

The established geochemical regularities are confirmed by the results of mineralogical studies. The relatively high-temperature formation of muscovite metasomatites under removal of silica and input of alkalis (mostly  $K_2O$ ) is accompanied by the formation of a specific paragenesis of accessory minerals: scheelite, zircon, monazite, fluorapatite, kesterite, W-rutile, thorite, and coffinite. Quartz–muscovite metasomatites, formed under low-temperature conditions with a less significant removal of  $SiO_2$  or, more seldom, its insignificant input and also with the input of  $K_2O$ , contain less newly formed minerals concentrating REE, W, Sn U, and Th. The prevailing accessory minerals are sulfides (pyrite, galena, chalcopyrite, and fahlores), which are responsible for the gold–metal signatures of these metasomatites.

The obtained results of geochemical and mineralogical analyses confirm the stages of metasomatic processes established earlier (Borodaevskii and Borodaevskaya, 1947) for the southern part of the Berezovskoe gold deposit. They show that a single metasomatic process at the early stages leads to the removal of a large amount of silica into the system, formation of solutions enriched in ore components, their subsequent crystallization under lower temperatures, and formation of quartz–sulfide veins and near-vein quartz–muscovite metasomatites.

We thank the staff of the Geological Directorate of the Berezovka Mine for assistance in geological research in the

workings of the Central and Northern mines. We are also grateful to D.A. Khanin (Institute of Experimental Mineralogy, Chernogolovka) and V.A. Shishlov and V.L. Kudryashov (Central Laboratory of the Russian Geological Research Institute, St. Petersburg) for help in analyses and to Prof. A.V. Kozlov (St. Petersburg Mining University) for the full discussion of the research results and for useful criticism.

This work was carried out within the framework of the budget project AAAA-A18-118052590032-6 (“Paleogeodynamics and evolution of structure-chemical complexes during the formation of continental crust (by the example of the Ural–Mongolian Orogenic Belt and the West Siberian Platform”) of the state assignment of the Institute of Geology and Geochemistry UB RAS.

## REFERENCES

- Baksheev, I.A., Belyatskii, B.V., 2011. Sm–Nd and Rb–Sr isotope systems of scheelite of the Berezovskoe gold deposit (Middle Urals). *Litosfera*, No. 4, 110–118.
- Baksheev, I.A., Prokof'ev, V.Yu., Ustinov, V.I., 2001. Genesis of metasomatic rocks and mineralized veins at the Berezovskoe deposit, Central Urals: Evidence from fluid inclusion and stable isotopes. *Geochem. Int.* 39 (2), 129–144.
- Bellavin, O.V., Vagshal', D.S., Nirenshtein, V.A., 1970. The Shartash granite massif (Middle Urals) and associated gold mineralization. *Izvestiya Akad. Nauk SSSR. Ser. Geol.*, No. 6, 86–90.
- Borodaevskaya, M.B., 1944. The origin of beresites and some other metasomatic rocks of the Berezovskoe gold deposit (Middle Urals). *Zapiski VMO* 73 (2), 123–141.
- Borodaevskii, N.I., Borodaevskaya, M.B., 1947. The Berezovskoe Ore Field [in Russian]. Metallurgizdat, Moscow.
- Bortnikov, N.S., Sazonov, V.N., Vikent'eva, O.V., Vikent'ev, I.V., Murzin, V.V., Naumov, V.B., Nosik, L.P., 1998. The role of magmatogenic fluid in the formation of the Berezovskoe mesothermal gold–quartz deposit, Urals. *Dokl. Akad. Nauk* 363 (1), 82–85.
- Chesnokov, B.V., 1973. Endogenous zoning of the Berezovskoe ore field (Middle Urals). *Dokl. Akad. Nauk SSSR* 210, 915–917.
- Chesnokov, B.V., Kotybaeva, N.N., Bushmakin, A.F., 1975. Endogenous bismuth and nickel minerals of the Berezovskoe gold deposit, Middle Urals, in: *Transactions of the Mining and Geological Institute of the Uralian Branch of the USSR* [in Russian]. Sverdlovsk, Issue 106, pp. 123–126.
- Chesnokov, B.V., Pokrovskii, P.V., Sandler, G.A., 1976. Variations in Ag contents in gold particles of the Berezovskoe ore field in connection with its endogenous zonation, in: *Transactions of the Sverdlovsk Mining Institute* [in Russian]. Sverdlovsk, Issue 124, pp. 108–111.
- Fershtater, G.B., 2013. Paleozoic Intrusive Magmatism in the Middle and South Urals [in Russian]. *Izd. RIO UrO RAN*, Yekaterinburg.
- Filimonov, S.V., 1999a. Bismuth and tellurium mineralization of gumbeyte association at the northern flank of the Berezovskoe gold deposit (Bi-tennantite, Ag–Bi-galena, aikinite, tetradymite, Pb-tetradymite, and hessite), in: *Uralian Summer Mineralogical School 1999* [in Russian]. UGGGA, Yekaterinburg, pp. 292–294.
- Filimonov, S.V., 1999b. The first finding of kesterite  $Cu_2(Zn,Fe)SnS_4$  and other In-containing minerals in the Berezovskoe gold deposit, in: *Uralian Summer Mineralogical School 1999* [in Russian]. UGGGA, Yekaterinburg, pp. 291–292.
- Filimonov, S.V., 2000. W-rutile from gumbeytes of the Berezovskoe gold ore field (Middle Urals), in: *Uralian Summer Mineralogical School 2000* [in Russian]. UGGGA, Yekaterinburg, pp. 376–378.
- Filimonov, S.V., 2009. Fahlore Group Minerals, Indicators of Ore Genesis (by the Example of Hydrothermal Gold Deposits). PhD Thesis [in Russian]. MGU, Moscow.

- Floyd, P.A., Winchester, J.A., 1975. Magma type and tectonic setting discrimination using immobile elements. *Earth Planet. Sci. Lett.* 27, 211–218.
- Ghaderi, M., Palin, J.M., Campbell, I.H., Sylvester, P.J., 1999. Rare earth element systematics in scheelite from hydrothermal gold deposits in the Kalgoorlie-Norseman region, Western Australia. *Econ. Geol.* 94, 423–438.
- Grabezhev, A.I., 1970. Specifics of beresitization of granitoids of the Shartash massif (Middle Urals). *Trudy GGI UFAN SSSR*, Issue 86, 10–14.
- Hart, C.J.R., Goldfarb, R.J., 2005. Distinguishing intrusion-related from orogenic gold systems. *New Zealand Minerals Conference Proceedings*, pp. 125–133.
- Kalugina, R.D., Kopanov, V.F., Storozhenko, E.V., Lukin, V.G., Stepanov, A.E., Rapoport, M.S., Il'yasova, G.A., Suslov, D.L., Mikhailova, E.N., Shub, I.Z., Glazyrina, N.S., Stratovich, V.I., Chernyak, Z.B., Mikhailov, A.P., Gerasimenko, B.N., 2017. State Geological Map of the Russian Federation, Scale of 1:200,000. Second ed. Middle Urals Series. Sheet O-41-XXV. Explanatory Note [in Russian]. Moskovskii Filial FGUBU "VSEGEI", Moscow.
- Karpinskii, A.P., 1887. Major typical rocks enclosing vein gold deposits in the Berezovka mountainous district. *Izvestiya Geologicheskogo Komiteta* 6 (7), 475–478.
- Kołodziejczyk, J., Pršek, J., Voudouris, P., Melfos, V., Asllani, B., 2016. Sn-bearing minerals and associated sphalerite from lead–zinc deposits, Kosovo: An electron microprobe and LA-ICP-MS study. *Minerals* 6 (2), p. 42, <https://doi.org/10.3390/min6020042>.
- Kurulenko, R.S., 1977. The history of formation of granitoids of the Shartash massif, in: *Yearbook of the Institute of Geology and Geochemistry UB USSR AS*, 1976 [in Russian]. Sverdlovsk, pp. 39–41.
- Kurulenko, R.S., Trayanova, M.V., Kobuzov, A.S., Yablonskaya, L.V., 1984. Scheelite mineralization of quartz veins of the Shartash massif, in: *Yearbook of the Institute of Geology and Geochemistry USC USSR AS*, 1984 [in Russian]. Sverdlovsk, pp. 104–105.
- MacLean, W.H., Barrett, T.J., 1993. Lithogeochemical techniques using immobile elements. *J. Geochem. Explor.* 48 (2), 109–133.
- Maksimov, M.M., 1977. *An Essay on Gold* [in Russian]. Nedra, Moscow.
- McDonough, W.F., Sun, S.-S., 1995. The composition of the Earth. *Chem. Geol.* 120, 223–253.
- Moore, F., Howie, R.A., 1984. Tin-bearing sulphides from St Michael's Mount and Cligga Head, Cornwall. *Mineral. Mag.* 48, 389–96.
- Pavlishin, V.I., Yushkin, N.P., Popov, V.A., 1988. The Ontogenetic Method in Mineralogy [in Russian]. Naukova Dumka, Kiev.
- Pearce, J.A., Cann, J.R., 1971. Ophiolite origin investigated by discriminant analysis using Ti, Zr and Y. *Earth Planet. Sci. Lett.* 12, 339–349.
- Pitcaim, I.K., 2011. Background concentrations of gold in different rock types. *Appl. Earth Sci. (Trans. Inst. Min. Metall. B)* 120 (1), 31–38.
- Plyushchev, E.V., Shatov, V.V., Kashin, S.V., 2012. Metallogeny of Hydrothermal-Metasomatic Rocks [in Russian]. Izd. VSEGEI, St. Petersburg.
- Polenov, Yu.A., Ogorodnikov, V.N., Babenko, V.V., 2013. The Berezovskoe quartz vein gold deposit, a classical object of polychronous and polygenetic formation. *Litosfera*, No. 6, 39–53.
- Popov, V.A., 1970. The relative age and types of beresites of the Berezovskoe gold deposit, in: *Metamorphic Rocks of the Urals* [in Russian]. Izd. SGI, Sverdlovsk, pp. 93–95.
- Popov, V.A., 1971. Ontogeny of Quartz of the Berezovskoe Gold Deposit (Urals). PhD Thesis [in Russian]. DVNTs AN SSSR, Khabarovsk.
- Popova, V.I., Artem'ev, D.A., Kotlyarov, V.A., 2018. Zoning of the form and composition of pyrite crystals of the Berezovskoe gold deposit (Urals). *Mineralogiya* 4 (2), 42–54.
- Pribavkin, S.V., 2002. Mineral cadastre of the Shartash massif. *Vestnik UrO RMO*, No. 1, 107–128.
- Pribavkin, S.V., Montero, P., Bea, F., Fershtater, G.B., 2013. The U–Pb age and composition of rocks of the Berezovskoe gold ore field (Middle Urals). *Litosfera*, No. 1, 136–145.
- Pribavkin, S.V., Sustavov, S.G., Gotman, I.A., 2018. Bismuth sulfosalts of the Berezovka area: chemical composition and mineral assemblages. *Litosfera* 18 (3), 334–458.
- Rose, G., 1842. *Mineralogisch–Geognostische Reise Nach dem Ural, dem Altai und Kaspischen Meere*. Berlin, Vol. 1.
- Rubin, J.N., Henry, C.D., Price, J.G., 1993. Mobility of zirconium and other "immobile" elements during hydrothermal alteration. *Chem. Geol.* 110, 29–47.
- Rudnik, V.A., 1962. Determination of the quantitative change of substance during metasomatic processes. *Zapiski VMO* 91 (6), 683–689.
- Samartsev, I.T., Zakhvatkin, V.A., Kazimirskii, V.F., 1973. Zonation of the Berezovskoe gold deposit (Middle Urals). *Geologiya Rudnykh Mestorozhdenii* 15 (1), 110–117.
- Sazonov, V.N., 1984. Beresite–Listwänite Association and Hosted Mineralization [in Russian]. UrO AN SSSR, Sverdlovsk.
- Sazonov, V.N., Borodaevskii, N.I., 1980. Genesis of the Structures and Textures of Metasomatites of Beresite–Listwänite Association (Preprint) [in Russian]. UrNTs AN SSSR, Sverdlovsk.
- Sazonov, V.N., Vikent'eva, O.V., Ogorodnikov, V.N., Polenov, Yu.A., Velikanov, A.A., 2006. Rare-earth elements in columns of propylitization, albitization, and beresitization–listwänitization of rocks with different silica contents: evolution of distribution, factors for appearance, and practical value. *Litosfera*, No. 3, 108–124.
- Sazonov, V.N., Ogorodnikov, V.N., Polenov, Yu.A., 2009. The behavior of REE during a low- to medium-temperature hydrothermal process and their indicator role, by the example of metasomatic columns differentiated by the composition of educts (Urals). *Litosfera*, No. 4, 51–66.
- Schreiber, D.W., Fonboté, L., Lochmann, D., 1990. Geologic setting, paragenesis, and physicochemistry of gold quartz veins hosted by plutonic rocks in the Pataz region. *Econ. Geol.* 85, 1328–1347.
- Shagalov, E.S., Stepanov, S.Yu., Veretennikova, T.Yu., 2018. Mineralogy of the Berezovskoe gold deposit (Middle Urals): thorium and uranium sulfides and minerals, in: *The 24th All-Russian Scientific Conference "Uralian Mineralogical School 2018"*. Collection of Papers by Students, Postgraduates, and Scientists of Research Institute and by Geology College Professors [in Russian]. Al'fa Print, Yekaterinburg, pp. 252–260.
- Sillitoe, R.H., Thompson, J.F.H., 1998. Intrusion-related vein gold deposits: types, tectono-magmatic settings and difficulties of distinction from orogenic gold deposits. *Resour. Geol.* 48 (4), 237–250.
- Sklyarov, E.V., Gladkochub, D.P., Donskaya, T.V., Ivanov, A.V., Letnikov, E.F., Mironov, A.G., Barash, I.G., Bulanov, V.A., Silykh, A.I., 2001. Interpretation of Geochemical Data [in Russian]. Internet Inzhiniring, Moscow.
- Spiridonov, E.M., Nurmukhametov, F.M., Sidorova, N.V., Korotava, N.N., Kulikova, I.M., Polenov, Yu.A., Troshkina, A.N., 2013. Syngenetic zircon, monazite, xenotime, and fluorapatite of apopite–phlogopite–magnesite gumbites of the Berezovskoe gold deposit (Urals). *Novye Dannye o Mineralakh*, Issue 48, 37–56.
- Sustavov, S.G., 2002. Minerals of the Berezovskoe gold deposit, in: *Uralian Summer Mineralogical School 2001* [in Russian]. UGGGA, Yekaterinburg, pp. 80–94.
- Thompson, J.F.H., Sillitoe, R.H., Baker, T., Lang, J.R., Mortensen, J.K., 1999. Intrusion-related gold deposits associated with tungsten–tin provinces. *Mineral. Deposita*, No. 34, 323–334.
- Vikent'eva, O.V., Bortnikov, N.S., Vikentyev, I.V., Groznova, E.O., Lyubimtseva, N.G., Murzin, V.V., 2017. The Berezovsk giant intrusion-related gold–quartz deposit, Urals, Russia: Evidence for multiple magmatic and metamorphic fluid reservoirs. *Ore Geol. Rev.* 91, 837–863.